Antenna Selection for Space-Time Trellis Codes over Rayleigh Fading Channels

Abdollah Sanei

A Thesis

in

The Department

of

Electrical and Computer Engineering

Presented in Partial Fulfillment of the Requirements

for the Degree of Doctor of Philosophy

Concordia University

Montreal, Quebec, Canada

January 2006

Your file Votre référence
ISBN: 978-0-494-16292-7
Our file Notre référence
ISBN: 978-0-494-16292-7

Abstract

Antenna Selection for Space-Time Trellis Codes over Rayleigh Fading Channels

Abdollah Sanei, Ph.D.

Concordia University, 2006

Employing multiple antennas in multiple-input multiple-output (MIMO) communication systems has many advantages over systems employing single-transmit and single-receive antennas. The most important of these advantages is the tremendous increase in channel capacity. However, employing multiple antennas results in a significant increase in the system complexity, and hence cost, since each employed antenna requires a separate radio frequency (RF) chain. Antenna selection has been introduced recently as a means to alleviate this complexity. The main idea behind antenna selection is to select at the transmitter and/or receiver a good subset of the available antennas. By this, the number of required RF chains reduces to as few as the number of selected antennas, thereby reducing the system complexity and its cost. Antenna selection has been considered for both space-time trellis codes (STTCs) and orthogonal space-time block codes (STBCs) with favorable results. However, all works in this area considered a particular channel model, namely, quasi-static Rayleigh fading.

In this thesis, we consider receive antenna selection for STTCs for generalized

Rayleigh fading channels. Specifically, we derive explicit upper and lower bounds on the performance of STTCs with antenna selection over fast and block Rayleigh fading channels. The latter channel model is a good model for most wireless communication channels because it encompasses a wide range of mobility and data rates. For both channel models, we show that the diversity order deteriorates with antenna selection and it becomes proportional to the number of selected antennas and not the number of available antennas. However, having more antennas available, while keeping the number of selected antennas fixed, increases the coding gain, which naturally comes as a result of an increased average SNR due to antenna selection. This is unlike the case for quasi-static fading where the diversity order is maintained with antenna selection provided that the underlying STTC is full rank.

As for STBCs, it appears that the channel model has no impact on the resulting diversity order with antenna selection. It has been shown that the diversity order of STBCs with antenna selection is the same as that of the full complexity system. In light of the results of this thesis and existing results in this area, the conclusion is that, when antenna selection is considered, it is recommended to use STBCs when the channel is fast fading or block fading with high mobility (or low data rate). On the other hand, it is recommended to use STTCs with antenna selection when the channel is modeled by quasi-static fading or block fading with low mobility (or high data rate).

This dissertation is dedicated to
my beloved passed away mother,
my father who is the best friend of mine,
and my wife,
who patiently endured the hardship of life
during these years .

Acknowledgments

I would like to express my heartiest gratitude and appreciation to my supervisors, Dr. Yousef R. Shayan and Dr. Ali Ghrayeb, for their great guidance and advice. I consider myself extremely fortunate for having them as my advisors. During the years of my study period, they followed up my research and encouraged me for more progress.

I would like to thank the examining committee of this dissertation for their suggestions and comments, which always were a great help, during my study period.

I would like to appreciate the Administratives in Semnan University who provided me the opportunity of continuing my education by granting enough leave time to accomplish my study.

It is the time to appreciate all of the efforts, done by all of my teachers in my life, from kind elementary school teachers, to knowledgeable university professors. I admire their skills and sincerely thank all of them, one by one.

Finally, I acknowledge my dear family, my very good passed away mother, my father as the best adviser, my brothers, my brother in law, my sister, my sister in laws, my the best wife and my sweet children, Daniel and Diana.

Contents

List of Figures

List of Tables

List of Symbols

M	Number of receive antennas
N	Number of transmit antennas
r_t^j	Received signal at time t by antenna j
c_t^i	Transmitted signal at time t by antenna i
ω_t^j	Noise at receiver at time t
$\alpha_{i,j}(t)$	Subchannel fading coefficient
l	Length of one frame
e	Decoded codeword
c	Received codeword
$d(c,e)$	Euclidean distance between c and e
$C(t)$	Symbol−wise codeword difference matrix
$\lambda(t)$	Matrix eigenvalue at time t
μ	Number of erruneously decoded symbols
$\varphi(c,e)$	Set of the indices of the erruneously decoded symbols
L	Number of selected antennas

$Y_j(t)$	Amount of energy picked up by receiver j
$X_j(t)$	Ordered amount of energy at the j^{th} receive antenna
δ	Length of one block
η	Number of erruneously decoded blocks
$\psi(c,e)$	Set of the indices of the erruneously decoded blocks
K	Number of blocks in a frame
$r(k)$	Rank of block number k
$A(k)$	Block−wise codeword difference matrix

List of Acronyms

AWGN	Additive white Gaussian noise
BER	Bit error rate
BPSK	Binary phase shift keying
BS	Base station
CSI	Channel state information
EGC	Equal gain combining
FER	Frame error rate
MIMO	Multiple–input multiple–output
MRC	Maximum ratio combining
SNR	Signal–to–noise ratio
STBC	Space–time block code
STTC	Space–time trellis code
PEP	Pairwise error probabilty
TCM	Trellis coded modulation
RF	Radio frequency

Chapter 1

Introduction

1.1 Literature Review

The challenge of achieving reliable data transmission over wireless links has drawn much attention from the coding community in recent years. This challenge stems from the fact that, in a wireless environment, unlike other applications, achieving reliable communication becomes much more difficult due to the possibility that received signals from multipaths may add destructively, which, consequently, results in serious performance degradation. It has been shown that a key technique for achieving reliable communication over wireless links is to introduce *antenna diversity* into the system. Antenna diversity is achieved by employing spatially separated antennas at the transmitter and/or receiver. The main advantage of using multiple antennas is that they result in a drastic increase in the channel capacity, as shown by Telatar [1], and Foschini and Gans [2].

Inspired by the promised increase in capacity, a large number of papers have been published recently on the use of antenna diversity for achieving reliable communication over wireless links. These include the early work by Guey, *et al.* [3] in which they consider signal design techniques that exploit the diversity provided by employing multiple antennas at the transmitter. Then Tarokh, *et al.* introduced in 1998 [4] the class of *space-time trellis codes* (STTCs), which are very efficient for systems with multiple transmit and receive antennas. In [5], Alamouti introduced a very simple, and yet efficient, scheme which involves using two transmit antennas at the base station (BS) and one receive antenna at the other end of the downlink. A simple decoding algorithm based on a linear receiver was introduced for this scheme, which can be extended for an arbitrary number of receive antennas.

Motivated by the simplicity of the Alamouti scheme, Tarokh, *et al.* [6] generalized that scheme to an arbitrary number of transmit antennas, resulting in the so-called *space-time block codes* (STBCs). Since the discovery of space-time codes, many papers have appeared in the literature in which various space-time coding schemes were considered in an effort to maximize the diversity order and coding gain that can be achieved for a given number of transmit and receive antennas, see [7]−[11] and the references therein.

One of the drawbacks of using multiple antennas is the associated complexity. That is, the complexity from the fact that a separate Radio Frequency (RF) chain is required for every employed antenna, resulting in a significant increase in the implementation cost. In addition, in some cases, it may be prohibitively complex to use

many RF chains, such as the case in mobile phones. With this motivation, *antenna selection* has been introduced recently as a means to alleviate the complexity associated with using multiple antennas, while exploiting the diversity provided by such antennas [18]−[41].

The idea behind antenna selection centers around using only a subset of the available antennas in multiple-input multiple-output (MIMO) systems. The implication of this selection is that the number of RF chains required is reduced to as few as the number of selected antennas, thereby the deployment of MIMO systems would become less expensive and more feasible. Antenna selection at the transmitter and the receiver under certain channel conditions has been considered for STTCs and STBCs extensively.

In [18], the authors consider the joint transmit and receive antenna selection based on the second order channel statistics, which is assumed to be available to the transmitter. The authors in [19] consider antenna selection for low rank matrix channels where selection is performed only at the transmitter. In [20], antenna selection is considered only at the transmitter with the assumption that the channel statistics are available to the transmitter. In [21], the authors show that, for full-rank STTCs over quasi-static fading channels, the diversity order is the same as that of the full-complexity system. In [28], Molisch *et al.* study the effect of antenna selection from a channel capacity perspective. It is shown that only a small loss in capacity is suffered when the receiver uses a good subset of the available receive antennas. Other work related to antenna selection for STTC codes can be found in [22]−[30].

In [31]−[37], the authors consider antenna selection for STBCs at the transmitter. They show that the performance is improved by increasing the number of transmit antennas while keeping the number of selected antennas fixed. In [38], antenna selection is considered at the transmitter (with the full knowledge of the channel statistics) or at the receiver for orthogonal STBCs with particular emphasis on the Alamouti scheme [5]. The authors use outage probability analysis to argue that the spatial diversity, when the underlying space-time code is orthogonal, is maintained with antenna selection. In [39], explicit upper bounds on the bit error rate (BER) performance of orthogonal STBCs with receive antenna selection are derived, and it is shown that the diversity order is maintained. The performance bounds presented in [39] were extended, with similar conclusions, to the case when the STBC is concatenated with an outer channel code, such as a convolutional code or a trellis-coded modulation (TCM) code [40].

In all of the work done on antenna selection for STTCs, it is mistakenly assumed that the underlying channel is quasi-static Rayleigh fading, i.e., the channel is fixed for a very long time. This was the channel model initially assumed in [21]. The main result for this channel model was that the diversity order with antenna selection remains the same as that of the full complexity system, whereas the performance suffers some degradation due to a reduction in the average SNR resulting from antenna selection. Given the fact that quasi-static fading models very limited wireless applications, and preliminary simulation results showed that the diversity order of

STTCs with antenna selection is not maintained for fast fading channels, this motivated us to thoroughly investigate the performance of STTCs with antenna selection for generalized fading channels.

1.2 Contributions

The contributions of this thesis may be summarized as follows.

- We derive explicit, rigorous upper and lower bounds on the performance of STTCs with antenna selection over fast fading channels. We show that the diversity order deteriorates with antenna selection and becomes proportional to the number of selected antennas and not the number of available antennas, as was previously (intuitively) believed.

- We show that having more antennas at the receiver, while keeping the number of selected antennas fixed, results in additional coding gains. This is justified by the increase in the average SNR due to selecting the best antennas. However, such coding gains become marginal as the number of available antennas increases.

- We derive explicit, rigorous upper and lower bounds on the performance of STTCs with antenna selection over block fading channels. Block fading models the vast majority of wireless channels, where fast and quasi-static fading are special cases of block fading. We show that the diversity order with antenna selection is not maintained, similar to the fast fading case. We also show that

some coding gains can be achieved by adding more antennas while keeping the number of selected antennas fixed.

- We show that the deterioration in the diversity order due to antenna selection is attributed to the combined code structure and channel model. For example, when the mobility in the channel is moderate to slow, the performance curves suggest that the diversity order is maintained (or nearly maintained). As the mobility increases and the channel model approaches fast fading, it becomes apparent that, even at low SNR, the diversity order is not maintained.

- In contrast, the diversity order with antenna selection for orthogonal STBCs is maintained for all channels types. This is due to the code structure which makes the resulting diversity order with antenna selection channel-independent. However, although STBCs are very simple to design, they do not provide any coding gains as compared to STTCs. To compensate for this, a STBC may be concatenated with an outer channel code. But the consequence of adding an outer code is a reduction in the transmission rate due to the overhead added, which is not desirable. So the conclusion here is that, when antenna selection is to be considered, one may use STTCs when the channel is quasi-static fading or when the mobility is relatively slow. On the other hand, when the channel is fast fading or the mobility is relatively fast, one should not use STTCs, and should use STBCs concatenated with an outer channel code.

1.3 Organization

The remainder of the thesis is outlined as follows.

- In Chapter 2, we review some preliminaries and definitions, including fading channels, MIMO system model and a brief introduction to space-time coding and antenna selection.

- In Chapter 3, we examine the performance of antenna selection over fast Rayleigh fading channels. We first review the full-complexity system and then derive upper bounds on the system performance for the special case of selecting the best antenna, and for the general case of selecting the best L out of M available antennas. Several numerical examples and simulation results that support the mathematical analysis are also presented.

- In Chapter 4, upper bounds on the pairwise error probability of STTCs with antenna selection over block Rayleigh fading channel are derived. Several numerical examples and simulation results are also given.

- In Chapter 5, we conclude the work and suggest some ideas as potential future work.

Chapter 2

Background

2.1 Fading Channels

In a cellular mobile radio environment, the surrounding objects, such as houses, buildings or trees, act as reflectors of radio waves. These obstacles produce reflected waves with attenuated amplitude and phases. If a modulated signal is transmitted, multiple reflected waves of the transmitted signal will arrive at the receiving antenna from different directions with different propagation delays, which are called multipath waves. Due to the different arrival angles and times, the multipath waves at the receiver site have different phases. When they are collected by the receive antenna at any point in space, they may combine either in a constructive or destructive way, depending on the random phases. The sum of these multipath components forms a spatially varying standing wave field.

The mobile unit moving through the multipath field will receive a signal which

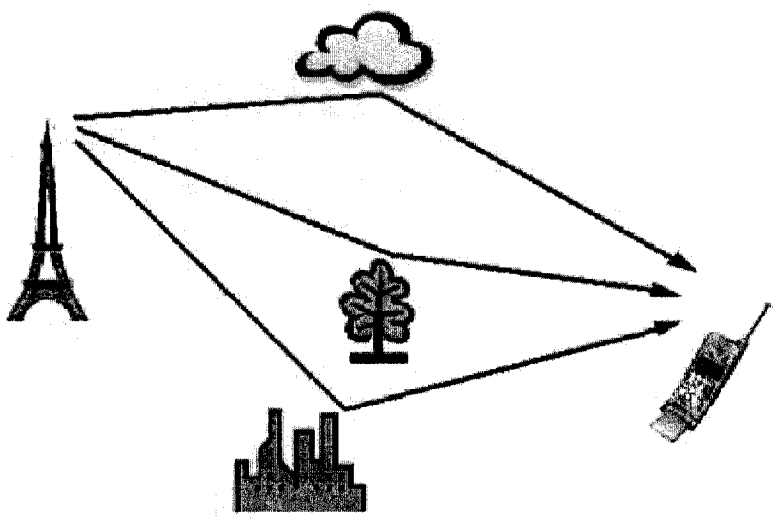

Figure 2.1: Mutipath fading channel.

can vary widely in amplitude and phase. When the mobile unit is stationary, the amplitude variations in the received signal are due to the movements of the surrounding objects in the radio channel. The amplitude fluctuation of the received signal is called signal fading. It is caused by the time-variant multipath characteristics of the channel.

In a narrowband system, the transmitted signals usually occupy a bandwidth smaller than the channel coherence bandwidth, which is defined as the frequency range over which the channel fading process is correlated. That is, all spectral components of the transmitted signals are subject to the same fading attenuation. This type of fading is referred to as frequency-nonselective (or flat). In a typical mobile radio channel, we may assume that the direct wave is obstructed and the mobile unit receives only reflected waves. Normally, Rayleigh fading model is used to model

the signal variations in narrowband multipath environment. When the number of reflected waves is large, according to the central limit theorem, the two quadrature components of the received signal are uncorrelated zero-mean Gaussian random processes. As a result, the envelope of the received signal at any time instant undergoes a Rayleigh probability distribution and its phase obeys a uniform distribution between $-\pi$ and $+\pi$. Assuming that average signal power ($E[|\alpha|^2]$) is unity, the normalized pdf for a Rayleigh distribution is written as $p(\alpha) = 2\alpha e^{-\alpha^2}$, for $\alpha \geqslant 0$.

On the other hand, when the received signal is made up of multiple reflective rays plus a significant nonfaded line-of-sight component, the received envelope amplitude has a Ricean probability density function as $p(\alpha) = 2\alpha e^{-(\alpha^2+K)} I_0(2\alpha K)$, for $\alpha, K \geqslant 0$, where K is the ratio of the power in nonfaded signal to the power in multipath signal and I_0 is the modified Bessel function of the first kind and zero order.

The impact of Rayleigh fading on the BER performance of Binary Phase Shift Keying (BPSK) is shown in Fig. 2.2. The figure compares the performance of the Rayleigh fading and additive white Gaussian noise (AWNG). It is clear from the figure that Rayleigh fading highly increases the bit error rate, which results in a huge deterioration in system performance.

Rayleigh fading can be either fast, block or slow, depending on the time variation of the channel, as well as the data rate. In fast fading, the channel fading coefficients (see Fig. 2.3) change at the beginning of each symbol interval and remain fixed during one symbol interval.

If the channel fading coefficients are constant during a fixed number of symbol

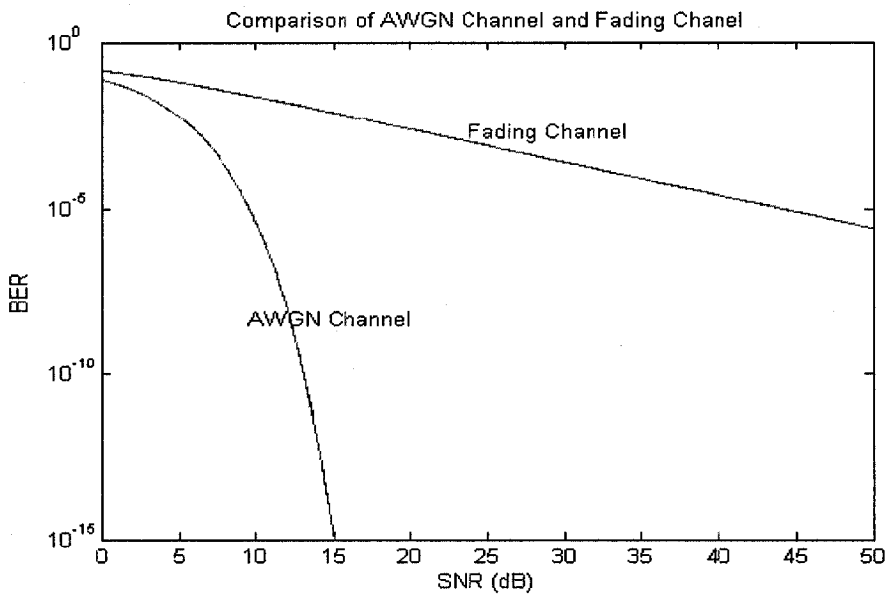

Figure 2.2: BER Performance of AWGN and fading channels [42].

intervals, which is shorter than the total transmission duration, i.e., frame duration, the channel is referred to as block fading. Finally, if the channel fading coefficients are constant during a frame and change from one frame to another, the channel is referred to as slow fading.

It has been shown that the most effective technique for combating fading is to introduce diversity into the system, which will be addressed in the next section.

2.2 Diversity

In wireless mobile communication systems, diversity techniques are widely used to reduce the effects of multipath fading and improve the reliability of transmission.

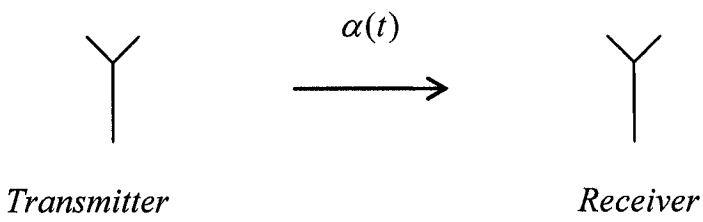

Figure 2.3: Channel fading coefficient.

Ideally, this performance improvement should be obtained without increasing the transmitted power or sacrificing the bandwidth. The diversity technique requires multiple replicas of the transmitted signals at the receiver, all carrying the same information but with small or no correlation in the fading statistics.

The basic idea of diversity is that, if two or more independent samples of the signal are taken, these samples will fade in an uncorrelated manner. This means that the probability of all the samples being simultaneously below a given level is much lower than the probability of any individual sample being below that level. Thus, a proper combination of the various samples results in great reduction of the fading impact, and correspondingly, improved reliability of transmission. In most wireless communication systems a number of diversity methods are used in order to get the required performance. Among these diversity techniques are temporal and spatial diversity, which are the two main diversity methods which are widely used in communication systems.

2.2.1 Temporal Diversity

Temporal diversity can be achieved by transmitting identical messages in different time slots, which results in uncorrelated fading signals at the receiver. In mobile communications, error control coding is combined with interleaving to achieve temporal diversity. In this case, the replicas of the transmitted signals are usually provided to the receiver in the form of redundancy in the time domain. The time separation between the replicas of the transmitted signals is provided by time interleaving to obtain independent fades. Since time interleaving results in decoding delay, this technique is usually effective for fast fading (high mobility) environments. For slow fading (low mobility) channels, a large interleaver can lead to a significant delay which is intolerable for delay sensitive applications such as voice transmission. One of the drawbacks of this scheme is that due to the redundancy introduced in the time domain, there is a loss in bandwidth.

2.2.2 Spatial Diversity

Spatial diversity, also called antenna diversity, has been a popular technique in wireless communications. This technique is typically implemented using multiple antennas for transmission and/or reception. The multiple antennas are separated physically by a proper distance, typically a few wavelengths, so that the individual signals are uncorrelated. In spatial diversity, the replicas of the transmitted signals are provided to the receiver in the form of redundancy in the space domain. Unlike temporal diversity, employing spatial diversity does not reduce the bandwidth

Figure 2.4: Simple examples of transmit and receive diversity.

efficiency. Depending on whether multiple antennas are used at the transmitter or receiver side, spatial diversity is classified into two categories: receive diversity and transmit diversity. Simple examples of transmit and receive diversity are shown in Fig. 2.4.

In receive diversity, multiple antennas are used at the receiver side to pick up independent copies of the transmit signals. The replicas of the transmitted signals are properly combined to increase the overall received SNR and mitigate the effect of multipath fading. Thus, if several paths have channel coefficients that are statistically independent, it is unlikely that they will fade together, so the probability of the signal strengths being below a certain detection threshold is small. In transmit diversity, multiple antennas are deployed at the transmitter side. Messages are processed at the transmitter and then spread across multiple antennas. Using transmit and/or receive diversity improves the system performance and reduces the system error rate. This

enhancement increases the slope of the error rate curve and shifts it towards regions of lower error rate. This can be explained, for example, by moving from the fading channel error rate curve towards the AWGN channel error rate curve, shown in Fig. 2.2.

2.3 MIMO Systems

A multiple input-multiple output (MIMO) system is a transmission system employing more than one antenna at each of the transmit and receive sides. Fig. 2.5 shows a typical model of MIMO system that has N transmit and M receive antennas. In each time interval, N signals are transmitted and each receive antenna receives the superposition of the faded transmitted signals. The channel is described by an $M \times N$ complex matrix as

$$\boldsymbol{\alpha}(t) = \begin{bmatrix} \alpha_{11}(t) & \alpha_{12}(t) & \cdots & \alpha_{1N}(t) \\ \alpha_{21}(t) & \alpha_{22}(t) & \cdots & \alpha_{2N}(t) \\ \vdots & \vdots & \ddots & \vdots \\ \alpha_{M1}(t) & \alpha_{M2}(t) & \cdots & \alpha_{MN}(t) \end{bmatrix}, \tag{2.1}$$

where, $\alpha_{i,j}(t)$, for $1 \leq i \leq N$, $1 \leq j \leq M$, $1 \leq t \leq l$, represent the channel fading coefficient from the i^{th} transmit to the j^{th} receive antenna. We assume that the channel is independent Rayleigh fading channel. As such, a signal transmitted from every individual transmit antenna appears uncorrelated at each of the receive

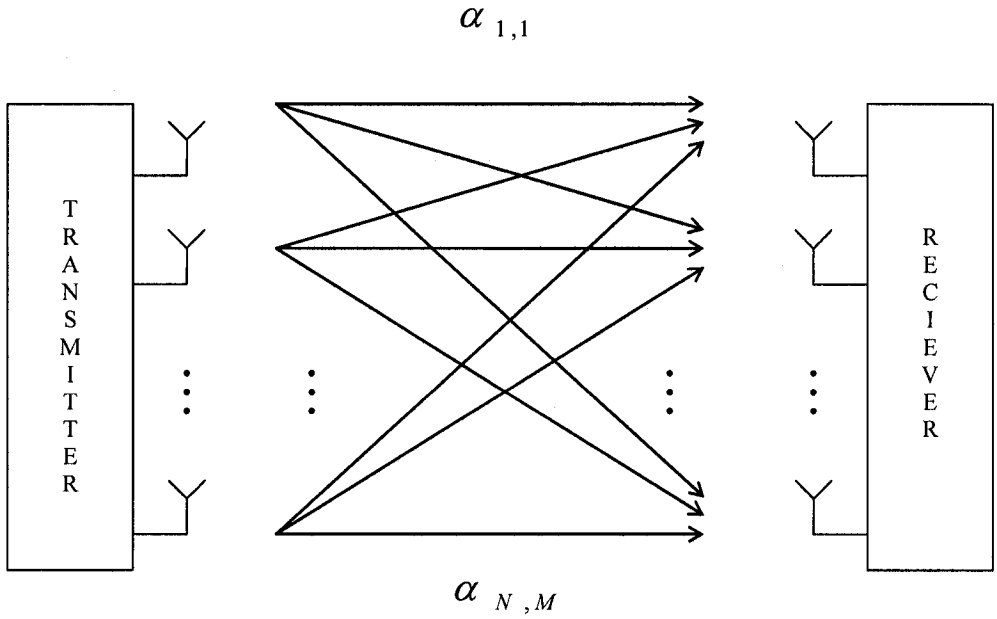

Figure 2.5: MIMO system model.

antennas. As a result, the signal corresponding to every transmit antenna has a distinct spatial signature at a receive antenna.

The assumption of independent Rayleigh fading results in uncorrelated Rayleigh distribution entries for the channel transfer matrix. The reason that we select the Rayleigh fading model is that Rayleigh models are realistic for environments with a large number of scatters, which is true for the most non-line-of-sight radio propagations. On the other hand, the independent fading model can be approximated where antenna elements spacing is considerably larger than the carrier wavelength, which is satisfied in many cases.

The noise at the receiver is described by the M independent complex zero mean

Gaussian random variables, with equal independent variance for the real and imaginary parts. Each of the M receive branches has identical noise power. The received signals are represented by M complex numbers, where each of them refers to a receive antenna.

2.4 Space-Time Coding

2.4.1 System Model

Space-time coding is a coding technique designed for use with multiple transmit antennas and is an effective practical way to approach the capacity of MIMO wireless channels. Coding is performed in both spatial and temporal domains to introduce correlation between signals transmitted from various antennas at various time intervals. Space-time coding can achieve transmit diversity as well as coding gain without sacrificing the bandwidth. There are various approaches in coding structure such as space-time trellis codes (STTCs) and space-time block codes (STBCs). Space-time coding can be further combined with multiple receive antennas to minimize the effects of multipath fading and to get closer to the capacity of MIMO systems.

Consider a wireless communication system equipped with N transmit and M receive antennas, which is shown in Fig. 2.6. As shown in the figure, the transmitted data is encoded by a space-time encoder. At each time instant t, a block of r binary symbols is fed into the space-time encoder. The encoder maps the binary symbol block into N modulation symbols from a signal set of 2^r points. The coded data are

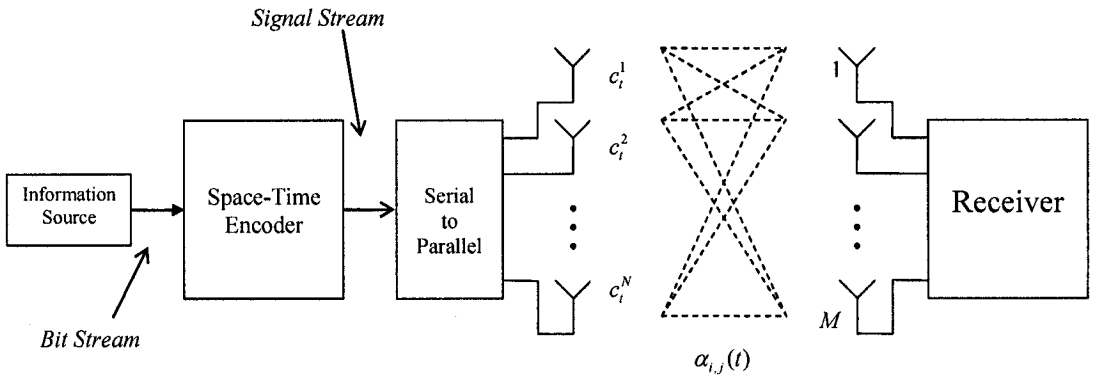

Figure 2.6: Space-time coding system model.

applied to a serial-to-parallel converter producing a sequence of N parallel symbols as

$$\mathbf{c} = c_1^1 c_1^2 \cdots c_1^N c_2^1 c_2^2 \cdots c_2^N \cdots c_l^1 c_l^2 \cdots c_l^N.$$

The N parallel outputs are simultaneously transmitted by N different antennas, whereby symbol c_t^i, $1 \leqslant i \leqslant N$, is transmitted by antenna i. The fading channel is described by a $M \times N$ channel transfer matrix, as expressed in (2.1). At the receiver, the signal at each of the M receive antennas is a noisy superposition of the N transmitted faded signals. At time t, the received signal at antenna j denoted by r_t^j, is given by

$$r_t^j = \sum_{i=1}^{N} \alpha_{i,j}(t) c_t^i + w_t^j, \tag{2.2}$$

where w_t^j is the noise component of receive antenna j at time t, which is an independent sample of the zero-mean complex Gaussian random variable with variance $N_0/2$ per dimension.

At the receiver, the decision metric is computed based on the squared Euclidean distance between the actual and hypothesized receive sequence as [4]

$$\sum_{t}\sum_{j=1}^{M}\left|r_t^j-\sum_{i=1}^{N}\alpha_{i,j}(t)c_t^i\right|^2, \tag{2.3}$$

where the decoder selects a codeword with the minimum decision metric as the decoded sequence.

2.4.2 Pairwise Error Probability

The pairwise error probability, $P(\mathbf{c}\rightarrow\ \mathbf{e})$, is the probability that the decoder selects an erroneous sequence $\mathbf{e}=e_1^1e_1^2\cdots e_1^Ne_2^1e_2^2\cdots e_2^N\cdots e_l^1e_l^2\cdots e_l^N$ over the transmitted sequence is $\mathbf{c}=c_1^1c_1^2\cdots c_1^Nc_2^1c_2^2\cdots c_2^N\cdots c_l^1c_l^2\cdots c_l^N$. The pairwise error probability conditioned on $\boldsymbol{\alpha}(t)$ in (2.1), is given by [4]

$$P(\mathbf{c}\rightarrow\ \mathbf{e}|\ \boldsymbol{\alpha}(\mathbf{t}))=\frac{1}{2}erfc\left(\sqrt{\frac{E_s}{4N_0}d^2(\mathbf{c},\mathbf{e})}\right), \tag{2.4}$$

where

$$d^2(\mathbf{c},\mathbf{e})=\sum_{t=1}^{l}\sum_{j=1}^{M}\left|\sum_{i=1}^{N}\alpha_{i,j}(t)\left(c_t^i-e_t^i\right)\right|^2. \tag{2.5}$$

The expression (2.4) can be easily simplified as

$$P(\mathbf{c} \rightarrow \mathbf{e} \mid \boldsymbol{\alpha}) \leq e^{\left(-d^2(\mathbf{c},\mathbf{e})E_s/4N_0\right)}, \tag{2.6}$$

which is an upper bound on the conditional pairwise error probability given by (2.4).

2.4.3 Diversity Gain and Coding Gain

By definition, the diversity gain is an approximate measure of the power gain of the system with space diversity over the system without diversity at the same error rate probability. The coding gain measures the power gain of the coded system over an uncoded system with the same diversity and the same error probability. As we will see later the diversity gain determines the slope of an error rate curve plotted as a function of SNR ratio, while the coding gain determines the horizontal shift of the uncoded system error rate curve to the space-time coded error rate curve obtained for the same diversity order. To explain more the idea of diversity gain and coding gain, we bring here two examples. In both examples it is assumed that the MIMO system has N transmit and M receive antennas, respectively.

In the first example, the upper bound on the PEP for space-time coded system working over slow Rayleigh fading channel is shown as [4]

$$P(\mathbf{c} \rightarrow \mathbf{e}) \leq \left(\prod_{i=1}^{r} \lambda_i\right)^{-M} \left(\frac{E_s}{4N_0}\right)^{-rM}. \tag{2.7}$$

In (2.7), r and λ are, respectively, the rank and eigenvalues of $A(\mathbf{c}, \mathbf{e})$ with entries

$A_{pq} = x_p x_q$, where $x_p = (c_1^p - e_1^p, c_2^p - e_2^p, \ldots, c_l^p - e_l^p)$ for $1 \leqslant p, q \leqslant N$. For this system, the diversity and coding gain are defined as rM and $(\lambda_1 \lambda_1 \cdots \lambda_1)^{\frac{1}{r}}$, respectively. Another example is the upper bound on the PEP for space-time coded system working over fast Rayleigh fading channel given as [4]

$$P(\mathbf{c} \rightarrow \mathbf{e}) \leq \left(\prod_{t \in \varphi(\mathbf{c},\mathbf{e})} |\mathbf{c}_t - \mathbf{e}_t|^2 \right)^{-M} \left(\frac{E_s}{4N_0} \right)^{-\mu M}, \tag{2.8}$$

where $\varphi(\mathbf{c}, \mathbf{e})$ denotes the set of time instances $1 \leq t \leq l$ such that $|\mathbf{c}_t - \mathbf{e}_t| \neq 0$ and $\mu = |\varphi(\mathbf{c}, \mathbf{e})|$ denote the size of $\varphi(\mathbf{c}, \mathbf{e})$. Here, the diversity gain achieved is μM and the coding gain is $\left(\prod_{t \in \varphi(\mathbf{c},\mathbf{e})} |\mathbf{c}_t - \mathbf{e}_t|^2 \right)^{\frac{1}{\mu}}$.

It is easy to see that in both cases, the variation of the diversity gain changes the slope of the error rate curve, while for the change of coding gain we observe a horizontal shift in the error rate curve.

2.5 Antenna Selection

In MIMO systems, the receiver sees several versions of the transmitted signal, each experiencing a different complex-valued fading coefficient $\alpha_{i,j}(t)$ and noise w_t^j. To exploit diversity, these signals must be combined in a gainful manner. Diversity combining can be classified into three categories. Selection diversity chooses the path with the highest SNR, and performs detection based on the signal from the selected path. Maximal ratio combining (MRC) makes decisions based on an optimal linear combination of the path signals. Equal gain combining (EGC) simply adds the path

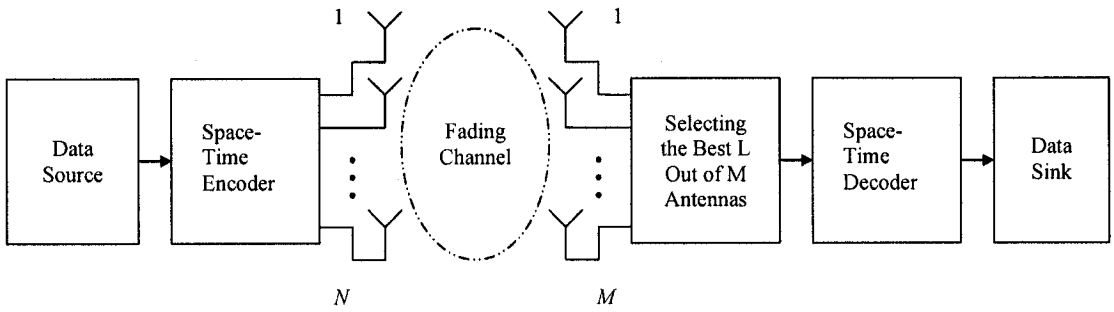

Figure 2.7: Antenna selection system.

signals after they have been cophased.

In this work, our concern is to evaluate the impact of employing antenna selection based on the selection diversity technique at the receiver side. From now on in this thesis, we use the short term of antenna selection to refer to the antenna selection system based on selection diversity, as shown in Fig. 2.7.

The main advantage of antenna selection is a reduction in the cost and complexity of the system. Ideally, a receive system with multiple antennas can improve the reliability of wireless communication. However, the multiple RF chains associated with multiple antennas are costly in terms of size, power, and hardware. Antenna selection is a low-cost, low-complexity alternative to capture many of the advantages of MIMO systems. As shown in Fig. 2.7, the selection block chooses only L out of the available M receive antennas, where $1 \leqslant L \leqslant M$. As a result, the number of RF chains required is reduced from M to L, as shown in Fig. 2.8 (The same thing can be done at the transmitter).

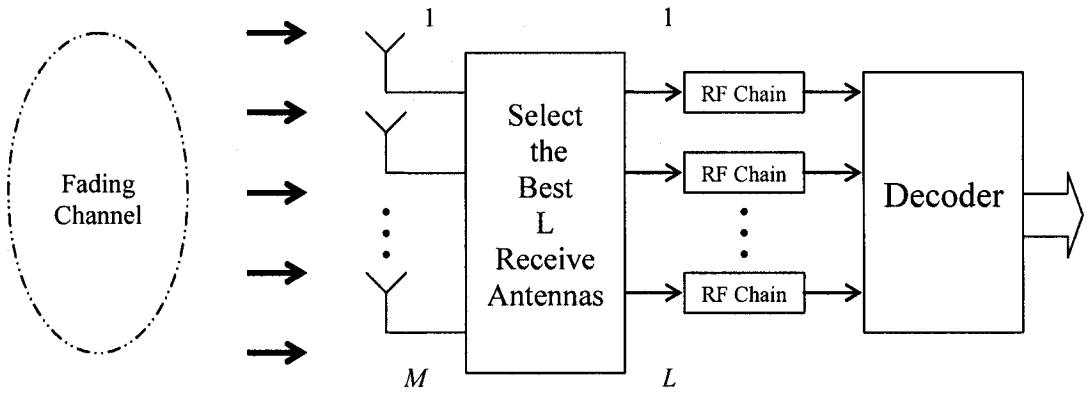

Figure 2.8: Selecting the best L antennas.

On the other hand, there are some drawbacks for employing antenna selection. For example, selection diversity techniques require knowledge of the channel conditions at the receiver for receive selection. Therefore, the performance of selection diversity will suffer if the channel state does not remain stationary, or if the estimate of channel state is inaccurate. Very little work has been done in characterizing the performance of antenna selection in the presence of time variations or noisy channel estimates [43].

Another example of the drawbacks for using antenna selection is the path independence assumption. The basic calculations for diversity reception often assume independent paths, but in practice the paths may be correlated, which reduces the effectiveness of selection diversity.

In this work, we are focused on evaluating the system performance of MIMO STTC antenna selection system. Some work has been accomplished to evaluate the performance of the space-time trellis coded MIMO antenna selection system working

over slow Rayleigh fading channel [21]. Based on this work, the diversity order of the antenna selection system that chooses a subset of the antennas with the highest SNR is the same as the diversity order of the full-complexity system, that is, using all of the receive antennas. Moreover, for slow fading, it has been shown that although the diversity order is maintained, the coding gain of the antenna selection system is less than the coding gain of the similar full-complexity system.

Chapter 3

Antenna Selection for Fast Fading Channels

3.1 Introduction

In this chapter, we consider receive antenna selection for STTCs over fast fading channels, where the channel coefficients fade independently from one symbol to the next. Such a model is suitable for a fully interleaved flat fading channel where an interleaver of length longer than the coherence time of the channel is employed. This may be done to make sure that the consecutive symbols transmitted see almost independent fades in an attempt to improve the error rate performance. Another scenario for this model is a frequency hopping system, where the consecutive symbols are transmitted using different carriers. Therefore, performing antenna selection in these scenarios is feasible since the selection is done at a rate lower than the symbol

rate.

We derive explicit upper bounds on the pairwise error probability for STTCs with receive antenna selection over fast Rayleigh fading channels. In performing antenna selection, we adopt a selection criterion that is based on selecting L out of the available M receive antennas that result in maximizing the instantaneous received SNR. We provide numerical examples and simulation results that validate these theoretical findings.

The rest of the chapter is outlined as follows. In Section 3.2, some results for the full-complexity systems related to our work are reviewed. In Section 3.3, we derive upper bounds on the PEP for STTCs with receive antenna selection. In Section 3.4 we provide numerical examples and simulation results that support our analysis. Finally, we conclude the chapter in Section 3.5.

3.2 Preliminaries

3.2.1 System Model

Consider a wireless communication system that employs N antennas at the transmitter side and M antennas at the receiver side (see Fig. 3.1). The incoming data is encoded by the space-time encoder. The output of the encoder is then fed into a serial-to-parallel converter that converts the input stream into N parallel streams. The resulting N streams are transmitted from the N transmit antennas simultaneously. At the receiver, after demodulation, matched-filtering, and sampling, the

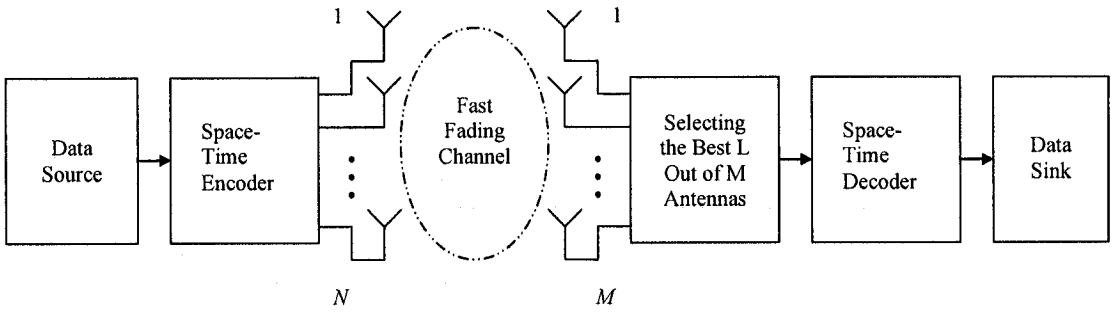

Figure 3.1: System model.

signal r_t^j received by antenna j at time t is given by

$$r_t^j = \sum_{i=1}^{N} \alpha_{i,j}(t) c_t^i + w_t^j, \tag{3.1}$$

where c_t^i is the signal transmitted from antenna i at time t; w_t^j is modeled as independent samples of a zero-mean complex Gaussian random variable with variance $N_0/2$ per dimension. The coefficients $\alpha_{i,j}(t)$ for $i = 1, 2, \ldots, N$, $j = 1, 2, \ldots, M$, and $t = 1, 2, \ldots, l$ model fading between the i^{th} transmit and j^{th} receive antennas at time t and are assumed to be complex Gaussian random variables with variance 0.5 per dimension. The fading coefficients $\alpha_{i,j}(t)$ change independently from one symbol to the next, which can be accomplished by interleaving. Furthermore, the subchannels are assumed to fade independently.

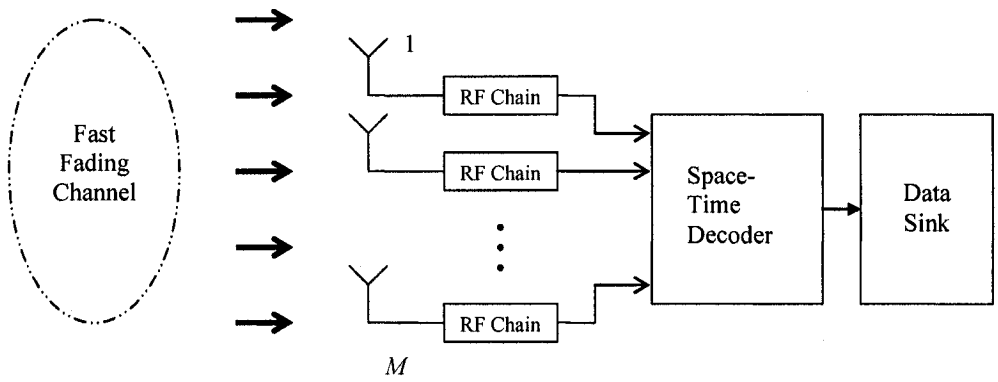

Figure 3.2: Full-complexity system.

3.2.2 Diversity Order of the Full-Complexity System

An upper bound on the PEP for STTCs over fast flat fading channels is derived in [4]. In this section, we review some definitions and highlight some of the main results reported in [4] which are relevant to our work. Here, the term full-complexity system, with a system model shown in Fig. 3.2, refers to a MIMO system that uses all available antennas.

Assuming maximum-likelihood decoding and that the channel state information (CSI) is perfectly known at the receiver, the conditional PEP that the receiver decides erroneously on the codeword

$$\mathbf{e} = e_1^1 e_1^2 \cdots e_1^N e_2^1 e_2^2 \cdots e_2^N \cdots e_l^1 e_l^2 \cdots e_l^N,$$

given that the codeword

$$\mathbf{c} = c_1^1 c_1^2 \cdots c_1^N c_2^1 c_2^2 \cdots c_2^N \cdots c_l^1 c_l^2 \cdots c_l^N$$

has been transmitted conditioned on the channel gains is upper bounded by

$$P(\mathbf{c} \rightarrow \mathbf{e} \mid \boldsymbol{\alpha}) \leq e^{\left(-d^2(\mathbf{c},\mathbf{e})E_s/4N_0\right)}, \tag{3.2}$$

where $\boldsymbol{\alpha} = \{\alpha_{i,j}(t) : 1 \leq i \leq N,\ 1 \leq j \leq M,\ 1 \leq t \leq l\}$ and

$$d^2(\mathbf{c},\mathbf{e}) = \sum_{t=1}^{l} \sum_{j=1}^{M} \left| \sum_{i=1}^{N} \alpha_{i,j}(t) \left(c_t^i - e_t^i\right) \right|^2, \tag{3.3}$$

where l denotes the length of the frame. After some simple manipulations, (3.3) can be rewritten as

$$d^2(\mathbf{c},\mathbf{e}) = \sum_{t=1}^{l} \sum_{j=1}^{M} \Omega_j(t) C(t) \Omega_j^*(t), \tag{3.4}$$

where $\Omega_j(t) = (\alpha_{1,j}(t), \ldots, \alpha_{N,j}(t))$, $C(t)_{pq} = (c_t^p - e_t^p)\overline{(c_t^q - e_t^q)}$ for $p, q = 1, \ldots, N$.

Since the matrix $C(t)$ is Hermitian, it can be factored as $C(t) = V(t)D(t)V^*(t)$ where $V(t)$ is a unitary matrix and $D(t)$ is a diagonal matrix with real-valued eigenvalues denoted by $\lambda_i(t)$ for $i = 1, 2, \ldots, N$ [44]. Now let

$$(\beta_{1,j}(t), \beta_{2,j}(t), \cdots, \beta_{N,j}(t)) = \Omega_j(t) V(t), \tag{3.5}$$

then $\beta_{i,j}(t)$ for $1 \leq i \leq N,\ 1 \leq j \leq M,\ 1 \leq t \leq l$, which can be put in a matrix form as

$$\boldsymbol{\beta}(t) = \begin{bmatrix} \beta_{11}(t) & \beta_{12}(t) & \dots & \beta_{1M}(t) \\ \beta_{21}(t) & \beta_{22}(t) & \dots & \beta_{2M}(t) \\ \vdots & \vdots & \ddots & \vdots \\ \beta_{N1}(t) & \beta_{N2}(t) & \dots & \beta_{NM}(t) \end{bmatrix}, \tag{3.6}$$

are independent complex Gaussian random variables with zero mean and variance 0.5 per dimension [4]. Consequently, we have

$$\Omega_j(t) C(t) \Omega_j^*(t) = \sum_{i=1}^{N} |\beta_{i,j}(t)|^2 \lambda_i(t). \tag{3.7}$$

Thus, (3.4) can be expressed as

$$d^2(\mathbf{c}, \mathbf{e}) = \sum_{t=1}^{l} \sum_{j=1}^{M} \sum_{i=1}^{N} |\beta_{i,j}(t)|^2 \lambda_i(t), \tag{3.8}$$

where $|\beta_{i,j}(t)|$ are Rayleigh distributed random variables with probability density function

$$p\left(|\beta_{i,j}(t)|\right) = 2\,|\beta_{i,j}(t)|\, e^{\left(-|\beta_{i,j}(t)|^2\right)}. \tag{3.9}$$

Averaging the expression in (3.2) with respect to the random variables $|\beta_{i,j}(t)|$

yields

$$P(\mathbf{c} \to \mathbf{e}) \leq \prod_{t=1}^{l} \prod_{j=1}^{M} \prod_{i=1}^{N} \int 2\,|\beta_{i,j}(t)|\, e^{\left(-|\beta_{i,j}(t)|^2\right)} \cdot e^{\left(-\frac{E_s}{4N_0}|\beta_{i,j}(t)|^2 \lambda_i(t)\right)} d\,|\beta_{i,j}(t)|\,, \quad (3.10)$$

which, after some simple manipulations, yields

$$P(\mathbf{c} \to \mathbf{e}) \leq \prod_{t=1}^{l} \prod_{i=1}^{N} \left(1 + \lambda_i(t) \frac{E_s}{4N_0}\right)^{-M}. \quad (3.11)$$

By examining the matrix $C(t)$, it is easy to see that the columns of this matrix are all multiples of

$$\mathbf{c}_t - \mathbf{e}_t = \left(c_t^1 - e_t^1, \ldots, c_t^N - e_t^N\right).$$

Therefore, the rank of $C(t)$ is 1 when $|\mathbf{c}_t - \mathbf{e}_t| \neq 0$ and 0 otherwise. When the rank is 1, it follows that, except for one of the eigenvalues, the rest are all zero. This occurs when $|\mathbf{c}_t - \mathbf{e}_t| \neq 0$. Let $\varphi(\mathbf{c}, \mathbf{e})$ denote the set of time instances $1 \leq t \leq l$ such that $|\mathbf{c}_t - \mathbf{e}_t| \neq 0$ and let $\mu = |\varphi(\mathbf{c}, \mathbf{e})|$ denote the size of $\varphi(\mathbf{c}, \mathbf{e})$. Then (3.11) simplifies to

$$P(\mathbf{c} \to \mathbf{e}) \leq \left(\prod_{t \in \varphi(\mathbf{c},\mathbf{e})} |\mathbf{c}_t - \mathbf{e}_t|^2\right)^{-M} \left(\frac{E_s}{4N_0}\right)^{-\mu M}, \quad (3.12)$$

which is an upper bound on the PEP and suggests that the diversity order of the full complexity system is μM. We use this diversity order as a baseline for the diversity

order achieved when antenna selection is employed. We remark that μ represents the minimum symbol-wise Hamming distance, which is directly related to the shortest error event length in the code trellis.

3.3 Upper Bounds on the PEP with Antenna Selection

In this section, we derive upper bounds on the PEP performance with antenna selection at the receiver. That is, the case when the receiver uses only L out of the available M receive antennas, where $1 \leqslant L \leqslant M$. Clearly, there are $\binom{L}{M}$ subsets to choose from, but as mentioned above, we assume that the selected subset is the one that results in the maximum instantaneous SNR at the receiver. We first start with the case $L = 1$, i.e., when the receiver selects the best antenna, and then generalize our analysis to an arbitrary number of selected antennas.

3.3.1 Selecting the Best Receive Antenna ($L = 1$)

Let us define $Y_j(t)$ as

$$Y_j(t) = \|\Omega_j(t)\|^2, \quad j = 1, 2, \ldots, M,$$

where $\|\cdot\|^2$ denotes the squared norm operator. Clearly, $Y_j(t)$ represents the amount of energy picked up by the j^{th} antenna at time instant t. Recall that when we select the

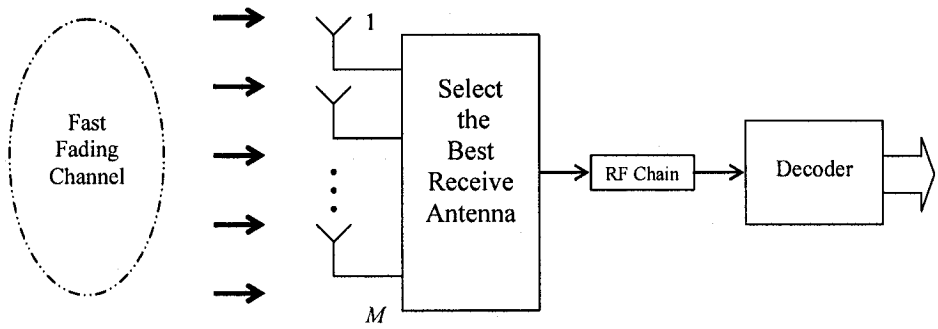

Figure 3.3: Antenna selection system, selecting the best antenna.

best antenna, each time we observe the sequence $Y_1(t), Y_2(t), \ldots, Y_M(t)$ and select the antenna corresponding to the largest term of this sequence. To simplify the analysis, we introduce a sequence of M auxiliary random variables, that we denote by $X_1(t), X_2(t), \ldots, X_M(t)$, such that $X_1(t) \geq X_2(t) \geq \cdots \geq X_M(t)$. This new sequence is obtained by arranging the random sequence $Y_1(t), Y_2(t), \ldots, Y_M(t)$ in an increasing order of magnitude. Furthermore, we may represent the random sequence $\Omega_1(t), \ldots, \Omega_M(t)$, after ordering, by the sequence $\Phi_1(t), \ldots, \Phi_M(t)$. Clearly, $X_j(t) = \|\Phi_j(t)\|^2$ for $j = 1, 2, \ldots, M$. When the best antenna is selected, expression (3.2) reduces to

$$\begin{aligned} P(\mathbf{c} \rightarrow \mathbf{e} \mid \Phi_1(t), t \in \{1, 2, \ldots, l\}) &\leq e^{\left(-\sum_{t=1}^{l}\left(\Phi_1(t)C(t)\Phi_1^*(t)\right)\frac{E_s}{4N_0}\right)} \\ &= \prod_{t=1}^{l} e^{\left(-\left(\Phi_1(t)C(t)\Phi_1^*(t)\right)\frac{E_s}{4N_0}\right)}. \end{aligned} \tag{3.13}$$

Note that $\Phi_1(t)$ is the vector of N complex Gaussian random variables

corresponding to the receive antenna with the largest instantaneous SNR at time t. Also, the random variables $\Phi_1(t)$, $t \in \{1, 2, \ldots, l\}$ are independent and identically distributed (iid). Now in order to find the average PEP, we average (3.13) with respect to the distribution of $\Phi_1(t)$. That is,

$$P(\mathbf{c} \rightarrow \mathbf{e}) \leq \prod_{t=1}^{l} \int_{\mathbb{C}^N} e^{\left(-\left(\phi_1(t)C(t)\phi_1^*(t)\right)\frac{E_s}{4N_0}\right)} f_{\Phi_1(t)}(\phi_1(t))\, d\phi_1(t), \tag{3.14}$$

where $\mathbb{C}^N$ denotes the $N-$dimensional complex space and $f_{\Phi_1(t)}(\phi_1(t))$ is the pdf of $\Phi_1(t)$ given by [45]

$$f_{\Phi_1(t)}(\phi_1(t)) = \frac{M}{\pi^N}\left(1 - e^{-\|\phi_1(t)\|^2}\sum_{i=0}^{N-1}\frac{\|\phi_1(t)\|^{2i}}{i!}\right)^{M-1} e^{-\|\phi_1(t)\|^2}. \tag{3.15}$$

Substituting (3.15) into (3.14) gives

$$P(\mathbf{c} \rightarrow \mathbf{e}) \leq \prod_{t=1}^{l} \frac{M}{\pi^N} \int_{\mathbb{C}^N} e^{\left(-\left(\phi_1(t)C(t)\phi_1^*(t)\right)\frac{E_s}{4N_0}\right)} \cdot \left(1 - e^{-\|\phi_1(t)\|^2}\sum_{i=0}^{N-1}\frac{\|\phi_1(t)\|^{2i}}{i!}\right)^{M-1} e^{-\|\phi_1(t)\|^2} d\phi_1(t). \tag{3.16}$$

By using the singular value decomposition of $C(t) = V(t)D(t)V^*(t)$ and the

change of variable $R(t) = \Phi_1(t)V(t)$, we can rewrite (3.16) as

$$P(\mathbf{c} \rightarrow \mathbf{e}) \leq \prod_{t=1}^{l} \frac{M}{\pi^N} \int_{\mathbb{C}^N} e^{\left(-\frac{E_s}{4N_0}\left(\sum_{i=1}^{N} |r_i(t)|^2 \lambda_i(t)\right)\right)} \cdot \left(1 - e^{-\|r(t)\|^2} \sum_{i=0}^{N-1} \frac{\|r(t)\|^{2i}}{i!}\right)^{M-1} e^{-\|r(t)\|^2} dr(t). \quad (3.17)$$

Further simplification of (3.17) is possible by applying the change of variable $r_i(t) = \rho_i(t)e^{j\theta_i(t)}$, which yields

$$P(\mathbf{c} \rightarrow \mathbf{e}) \leq \prod_{t=1}^{l} M 2^N \int_0^{\infty} \cdots \int_0^{\infty} e^{\left(-\frac{E_s}{4N_0}\left(\sum_{i=1}^{N} \rho_i^2(t)\lambda_i(t)\right)\right)} \cdot \left(1 - e^{-\sum_{i=1}^{N}\rho_i^2(t)} \sum_{i=0}^{N-1} \frac{\left(\sum_{i=1}^{N} \rho_i^2(t)\right)^i}{i!}\right)^{M-1} e^{-\sum_{i=1}^{N}\rho_i^2(t)} \left(\prod_{i=1}^{N} \rho_i(t)\right) d\rho_1(t) \cdots d\rho_N(t).$$

To simplify this expression further we note that if $y(x) = 1 - e^{-x}\sum_{i=0}^{N-1} \frac{x^i}{i!}$, then $y(x) \leq \frac{x^N}{N!}$ for $x > 0$ [11]. By using this result and defining $x = \sum_{i=1}^{N} \rho_i^2(t)$ and with the help of the change of variable $u_i(t) = \rho_i^2(t)$, we obtain

$$P(\mathbf{c} \rightarrow \mathbf{e}) \leq \prod_{t=1}^{l} \frac{M}{(N!)^{M-1}} \int_0^{\infty} \cdots \int_0^{\infty} e^{\left(-\sum_{i=1}^{N} u_i(t)\left(\frac{E_s}{4N_0}\lambda_i(t)+1\right)\right)} \cdot \left(\sum_{i=1}^{N} u_i(t)\right)^{(M-1)N} du_1(t) \cdots du_N(t), \quad (3.19)$$

where

$$\left(\sum_{i=1}^{N} u_i(t)\right)^{(M-1)N} = \sum_{i_1=1}^{N} \cdots \sum_{i_{(M-1)N}=1}^{N} u_{i_1}(t) \cdots u_{i_{(M-1)N}}(t)$$
$$= \sum_{i_1=1}^{N} \cdots \sum_{i_{(M-1)N}=1}^{N} \prod_{j=1}^{N} u_j^{k_j}(t), \tag{3.20}$$

and k_j represents the number of times the term $u_j(t)$ appears in the product

$$u_{i_1}(t)u_{i_2}(t)\cdots u_{i_{(M-1)N}}(t).$$

Note that $j \in \{1, 2, \ldots, N\}$, $k_j \in \{0, 1, \ldots, (M-1)N\}$, and $\sum_{j=1}^{N} k_j = (M-1)N$.

Substituting (3.20) into (3.19) yields

$$P(\mathbf{c} \to \mathbf{e}) \leq \prod_{t=1}^{l} \frac{M}{(N!)^{M-1}} \int_0^\infty \cdots \int_0^\infty e^{\left(-\sum_{i=1}^{N} u_i(t)\left(\frac{E_s}{4N_0}\lambda_i(t)+1\right)\right)}$$
$$\cdot \left(\sum_{i_1=1}^{N} \cdots \sum_{i_{(M-1)N}=1}^{N} \prod_{j=1}^{N} u_j^{k_j}(t)\right) du_1(t)\cdots du_N(t), \tag{3.21}$$

which can be rewritten as,

$$P(\mathbf{c} \to \mathbf{e}) \leq \prod_{t=1}^{l} \frac{M}{(N!)^{M-1}} \sum_{i_1=1}^{N} \cdots \sum_{i_{(M-1)N}=1}^{N} \int_0^\infty \cdots \int_0^\infty e^{\left(-\sum_{i=1}^{N} u_i(t)\left(\frac{E_s}{4N_0}\lambda_i(t)+1\right)\right)}$$
$$\cdot \left(\prod_{j=1}^{N} u_j^{k_j}(t)\right) du_1(t)\cdots du_N(t). \tag{3.22}$$

By using $\int_0^\infty x^k e^{-ax} dx = \frac{k!}{a^{k+1}}$, where $a = \frac{E_s}{4N_0}\lambda_i(t) + 1$, (3.22) can be expressed as

$$P(\mathbf{c} \to \mathbf{e}) \leq \prod_{t=1}^{l} \frac{M}{(N!)^{M-1}} \sum_{i_1=1}^{N} \cdots \sum_{i_{(M-1)N}=1}^{N} \prod_{j=1}^{N} \frac{k_j!}{\left(1 + \lambda_j(t)\frac{E_s}{4N_0}\right)^{k_j+1}}, \tag{3.23}$$

or equivalently,

$$P(\mathbf{c} \to \mathbf{e}) \leq \prod_{t=1}^{l} \frac{M}{(N!)^{M-1}} \sum_{i_1=1}^{N} \cdots \sum_{i_{(M-1)N}=1}^{N} \frac{k_1! \cdots k_N!}{\prod_{j=1}^{N} \left(1 + \lambda_j(t)\frac{E_s}{4N_0}\right)^{k_j+1}}. \tag{3.24}$$

Using the fact that, when $t \in \varphi(\mathbf{c}, \mathbf{e})$, the eigenvalues are all zero except for one, which we denote by $\lambda'(t)$, and for sufficiently large SNR, the term

$$\prod_{j=1}^{N} (1 + \lambda_j(t)\frac{E_s}{4N_0})^{k_j+1}$$

will tend to ∞ except when $k_j = 0$. As such, we can simplify (3.24) as

$$P(\mathbf{c} \to \mathbf{e}) \leq \left(\frac{M}{(N!)^{M-1}}\right)^{l} \prod_{t \in \varphi(\mathbf{c},\mathbf{e})} \left(\lambda'(t)\frac{E_s}{4N_0}\right)^{-1} \left(\sum_{i_1=1}^{N} \cdots \sum_{i_{(M-1)N}=1}^{N} k_1! \cdots k_N!\right). \tag{3.25}$$

Furthermore, the term $\sum_{i_1=1}^{N} \cdots \sum_{i_{(M-1)N}=1}^{N} k_1! \cdots k_N!$ in (3.25) is independent of t.

Therefore, we arrive at

$$P(\mathbf{c} \rightarrow \mathbf{e}) \leq \left(\frac{M}{(N!)^{M-1}}\right)^{l} K^{\mu}(M,N,1) \left(\prod_{t\in\varphi(\mathbf{c},\mathbf{e})} |\mathbf{c}_t - \mathbf{e}_t|^2\right)^{-1} \left(\frac{E_s}{4N_0}\right)^{-\mu}, \tag{3.26}$$

where $K(M,N,1) = \sum_{i_1=1}^{N} \cdots \sum_{i_{(M-1)N}=1}^{N} k_1! \cdots k_N!$. By comparing (3.26) and (3.12), it is clear that the diversity order reduces from μM to μ when the receiver selects the best antenna. However, since this result is only an upper bound on the PEP, it only shows that the diversity order cannot be worse than μ. In order to make a stronger argument, we still need to find a lower bound on the PEP to conclude that the diversity order indeed deteriorates as suggested by (3.26). To do this, we use Craig's expression for $Q(x)$ [47], that is,

$$Q(x) = \frac{1}{\pi} \int_0^{\frac{\pi}{2}} e^{\left(-\frac{x^2}{2\sin^2\theta}\right)} d\theta, \tag{3.27}$$

in order to find the lower bound on the system performance. By using Craig's formula, (3.27), we can write the conditional PEP when the best antenna is selected as

$$P(\mathbf{c} \rightarrow \mathbf{e} \mid \Phi_1(t), t \in \{1,2,\ldots,l\}) = \frac{1}{\pi} \int_0^{\frac{\pi}{2}} \prod_{t=1}^{l} e^{\left(-\left(\Phi_1(t)C(t)\Phi_1^*(t)\right)\frac{E_s}{8N_0\sin^2\theta}\right)} d\theta. \tag{3.28}$$

Averaging (3.28) with respect to $\Phi_1(t)$ and following the change of variables that

led to (3.18) yield

$$P(\mathbf{c} \rightarrow \mathbf{e}) = \frac{1}{\pi} \int_0^{\frac{\pi}{2}} \prod_{t=1}^{l} M 2^N \int_0^{\infty} \cdots \int_0^{\infty} e^{\left(-\frac{E_s}{8N_0 \sin^2 \theta} \left(\sum_{i=1}^{N} \rho_i^2(t) \lambda_i(t) \right) \right)}$$
$$\cdot \left(1 - e^{-\sum_{i=1}^{N} \rho_i^2(t)} \sum_{i=0}^{N-1} \frac{\left(\sum_{i=1}^{N} \rho_i^2(t) \right)^i}{i!} \right)^{M-1} e^{-\sum_{i=1}^{N} \rho_i^2(t)} \left(\prod_{i=1}^{N} \rho_i(t) \right) d\rho_1(t) \cdots d\rho_N(t) d\theta. \tag{3.29}$$

Expression (3.29) can be simplified further using the fact that if $y(x) = 1 - e^{-x} \sum_{i=0}^{N-1} \frac{x^i}{i!}$, then $y(x) \geqslant e^{-x} \frac{x^N}{N!}$ for $x > 0$ [11]. Using this result, (3.29) can be lower bounded as

$$P(\mathbf{c} \rightarrow \mathbf{e}) \geqslant \frac{1}{\pi} \int_0^{\frac{\pi}{2}} \prod_{t=1}^{l} M 2^N \int_0^{\infty} \cdots \int_0^{\infty} e^{\left(-\frac{E_s}{8N_0 \sin^2 \theta} \sum_{i=1}^{N} \rho_i^2(t) \lambda_i(t) \right)} e^{-\sum_{i=1}^{N} \rho_i^2(t)} \left(\frac{e^{-\sum_{i=1}^{N} \rho_i^2(t)}}{N!} \right)^{M-1}$$
$$\cdot \left(\sum_{i=1}^{N} \rho_i^2(t) \right)^{N(M-1)} \left(\prod_{i=1}^{N} \rho_i(t) \right) d\rho_1(t) \cdots d\rho_N(t) d\theta, \tag{3.30}$$

Using the change of variable $u_i(t) = \rho_i^2(t)$, we can rewrite (3.30) as

$$P(\mathbf{c} \rightarrow \mathbf{e}) \geqslant \frac{1}{\pi} \int_0^{\frac{\pi}{2}} \prod_{t=1}^{l} \frac{M}{(N!)^{M-1}} \int_0^{\infty} \cdots \int_0^{\infty} e^{\left(-\sum_{i=1}^{N} u_i(t) \left(\lambda_i(t) \frac{E_S}{8N_0 \sin^2 \theta} + M \right) \right)}$$
$$\left(\sum_{i=1}^{N} u_i(t) \right)^{N(M-1)} du_1(t) \cdots du_N(t) d\theta. \tag{3.31}$$

Following similar steps that led to (3.24), we can simplify (3.31) as

$$P(\mathbf{c} \rightarrow \mathbf{e}) \geqslant \frac{1}{\pi} \int_0^{\frac{\pi}{2}} \prod_{t=1}^{l} \frac{M}{(N!)^{M-1}} \sum_{g_1=1}^{N} \cdots \sum_{g_{(M-1)N}=1}^{N} \frac{k_1! \cdots k_N!}{\prod_{j=1}^{N} \left(M + \lambda_j(t) \frac{E_s}{8N_0 \sin^2\theta}\right)^{k_j+1}} d\theta. \tag{3.32}$$

We can express (3.32) as

$$P(\mathbf{c} \rightarrow \mathbf{e}) \geqslant \frac{1}{\pi} \int_0^{\frac{\pi}{2}} \prod_{t=1}^{l} \frac{M}{(N!)^{M-1}} \sum_{g_1=1}^{N} \cdots \sum_{g_{(M-1)N}=1}^{N} \frac{k_1! \cdots k_N!}{\prod_{j=1}^{N} M^{k_j+1} \prod_{j=1}^{N} \left(1 + \lambda_j(t) \frac{E_s}{8MN_0 \sin^2\theta}\right)^{k_j+1}} d\theta. \tag{3.33}$$

On the other hand, with the help of $\sum_{j=1}^{N} k_j = (M-1)N$ we can write

$$\begin{aligned} \prod_{j=1}^{N} M^{k_j+1} &= M^{-\sum_{j=1}^{N} k_j+1} \\ &= M^{-((M-1)N+N)} \\ &= M^{-MN}. \end{aligned} \tag{3.34}$$

Thus, we can write (3.33) as

$$P(\mathbf{c} \rightarrow \mathbf{e}) \geqslant \frac{1}{\pi} \int_0^{\frac{\pi}{2}} \prod_{t=1}^{l} \frac{1}{M^{NM-1}(N!)^{M-1}} \sum_{g_1=1}^{N} \cdots \sum_{g_{(M-1)N}=1}^{N} \frac{k_1! \cdots k_N!}{\prod_{j=1}^{N} \left(1 + \lambda_j(t) \frac{E_s}{8MN_0 \sin^2\theta}\right)^{k_j+1}} d\theta. \tag{3.35}$$

At a relatively large SNR and since there is only one nonzero eigenvalue when $t \in \varphi(\mathbf{c}, \mathbf{e})$, (3.35) can be expressed as

$$P(\mathbf{c} \to \mathbf{e}) \geqslant \frac{1}{\pi}\left(\frac{1}{M^{NM-1}(N!)^{M-1}}\right)^{l} \int_0^{\frac{\pi}{2}} \prod_{t\in\varphi(\mathbf{c},\mathbf{e})} \left(\sum_{g_1=1}^{N} \cdots \sum_{g_{(M-1)N}=1}^{N} k_1! \cdots k_N!\right) \cdot M^{-1}\left(\lambda'(t)\frac{E_s}{8N_0 \sin^2\theta}\right) d\theta, \quad (3.36)$$

which can be rewritten as

$$P(\mathbf{c} \to \mathbf{e}) \geqslant \frac{M^{\mu}}{\pi}\left(\frac{1}{M^{NM-1}(N!)^{M-1}}\right)^{l} K^{\mu}(N, M, 1)\left(\prod_{t\in\varphi(\mathbf{c},\mathbf{e})} |\mathbf{c}_t - \mathbf{e}_t|^2\right)^{-1} \cdot \left(\frac{E_s}{4N_0}\right)^{-\mu} \int_0^{\frac{\pi}{2}} \left(\frac{1}{2\sin^2\theta}\right)^{-\mu} d\theta. \quad (3.37)$$

Since the expressions on the right hand sides of (3.26) and (3.37) both have the same slope, we argue that the actual PEP has the same slope as well, which clearly shows that the diversity order achieved is μ. Therefore, the diversity order of the system is reduced from μM to μ when only the best antenna is selected at the receiver. An intuitive explanation for this result is given later.

3.3.2 Selecting More Than One Antenna ($L > 1$)

In this section, we generalize the result of the previous section to a system that selects the best L out of the total available M receive antennas, as shown in Fig. 3.4. When the receiver selects the best L antennas, the PEP defined by (3.2) can be

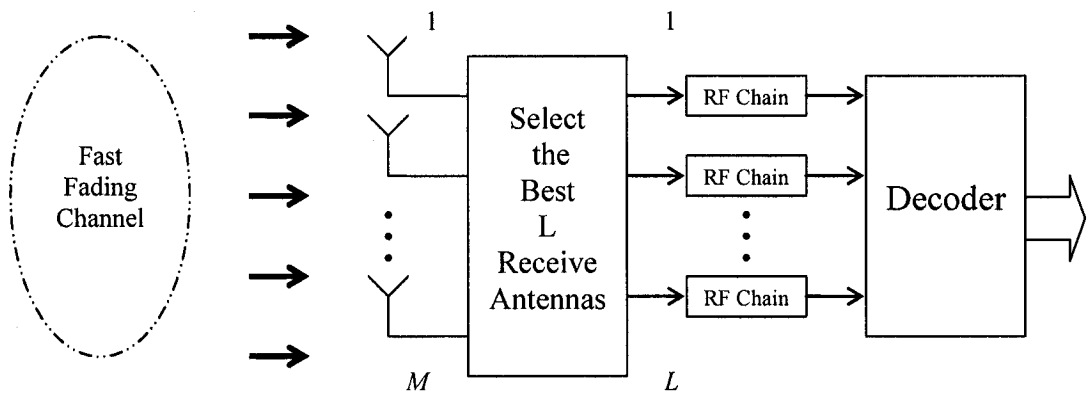

Figure 3.4: Antenna selection system, when the best L antennas are selected.

expressed as

$$P(\mathbf{c} \rightarrow \mathbf{e} \mid \Phi_1(t), \ldots, \Phi_L(t), t \in \{1, 2, \ldots, l\}) \leqslant e^{\left(-\sum_{t=1}^{l}\sum_{j=1}^{L}\left(\Phi_j(t)C(t)\Phi_j^*(t)\right)\frac{E_s}{4N_0}\right)}, \quad (3.38)$$

where it is assumed that $\|\Phi_1(t)\|^2 \geq \cdots \geq \|\Phi_L(t)\|^2$. Now to find an expression for the PEP, we need to average (3.38) with respect to the joint distribution of $\Phi_1(t), \ldots, \Phi_L(t)$ as follows.

$$P(\mathbf{c} \rightarrow \mathbf{e}) \leq \prod_{t=1}^{l} \int_{\Phi_L(t)} \cdots \int_{\Phi_1(t)} e^{\left(-\sum_{j=1}^{L}\left(\Phi_j(t)C(t)\Phi_j^*(t)\right)\frac{E_s}{4N_0}\right)} f_{\Phi_1(t),\ldots,\Phi_L(t)}(\phi_1(t), \ldots, \phi_L(t))\, d\phi_1(t) \cdots d\phi_L(t), \quad (3.39)$$

where $\Phi_j(t)$ is the vector of N complex Gaussian random variables corresponding to the receive antenna with the j^{th} largest instantaneous SNR, and

$$f_{\Phi_1(t),\cdots,\Phi_L(t)}\left(\phi_1(t),\ldots,\phi_L(t)\right)$$

is the joint pdf of $\Phi_1(t),\ldots,\Phi_L(t)$ given by [44]

$$f_{\Phi_1(t),\cdots,\Phi_L(t)}\left(\phi_1(t),\ldots,\phi_L(t)\right) = \frac{M!}{\pi^{NL}(M-L)!L!L} e^{-\sum_{j=1}^{L}\|\phi_j(t)\|^2} \cdot \left(\sum_{q=1}^{L}\left[1-e^{-\|\Phi_q(t)\|^2}\sum_{i=0}^{N-1}\frac{\|\phi_q(t)\|^{2i}}{i!}\right]^{M-L} I_{\Phi_q}(\phi_1(t),\ldots,\phi_L(t))\right), \quad (3.40)$$

where $I_{\Phi_q}\left(\phi_1(t),\phi_2(t),\ldots,\phi_L(t)\right) = 1$ if $\phi_1(t),\phi_2(t),\ldots,\phi_L(t) \in \Phi_q$ and 0 otherwise. Therefore, (3.39) becomes

$$P(\mathbf{c}\rightarrow\ \mathbf{e}) \leq \prod_{t=1}^{l}\frac{M!}{\pi^{NL}(M-L)!L!L} \cdot \int_{\Phi_L(t)}\cdots\int_{\Phi_1(t)} e^{\left(-\sum_{j=1}^{L}\left(\Phi_j(t)C(t)\Phi_j^*(t)\right)\frac{E_s}{4N_0}\right)} e^{-\sum_{j=1}^{L}\|\phi_j(t)\|^2} \cdot \left(\sum_{q=1}^{L}\left[1-e^{-\|\phi_q(t)\|^2}\sum_{i=0}^{N-1}\frac{\|\phi_q(t)\|^{2i}}{i!}\right]^{M-L}\right) d\phi_1(t)\cdots d\phi_L(t), \quad (3.41)$$

which is possible to be rewritten as

$$P(\mathbf{c} \rightarrow \mathbf{e}) \leq \prod_{t=1}^{l} \frac{M!}{\pi^{NL}(M-L)!L!^{L}} \sum_{q=1}^{L} \int_{\Phi_L(t)} \cdots \int_{\Phi_1(t)} e^{\left(-\sum_{j=1}^{L}\left(\Phi_j(t)C(t)\Phi_j^*(t)\right)\frac{E_s}{4N_0}\right)} e^{-\sum_{j=1}^{L}\|\phi_j(t)\|^2} \cdot \left[1 - e^{-\|\phi_q(t)\|^2} \sum_{i=0}^{N-1} \frac{\|\phi_q(t)\|^{2i}}{i!}\right]^{M-L} d\phi_1(t) \cdots d\phi_L(t). \quad (3.42)$$

To simplify the analysis, we perform the integration over the entire space, which results in a looser bound, but the diversity order remains unaffected. With this simplification, the $L-$fold integration can be broken down into a product of L integrations. This is possible due to the symmetry of the marginal pdfs of the random variables $\Phi_1(t), \ldots, \Phi_L(t)$. Each term of $\sum_{q=1}^{L}$ can be written as the multiplication of two factors for $k \neq q$ as

$$\Gamma_q = \left(\prod_{k=1}^{L} \int_{\Phi_k(t)} e^{\left(-\left(\Phi_k(t)C(t)\Phi_k^*(t)\right)\frac{E_s}{4N_0}\right)} e^{-\|\phi_k(t)\|^2} d\phi_k(t)\right) \cdot \left(\int_{\Phi_q(t)} e^{\left(-\left(\Phi_q(t)C(t)\Phi_q^*(t)\right)\frac{E_s}{4N_0}\right)} e^{-\|\phi_q(t)\|^2} \left(1 - e^{-\|\phi_q(t)\|^2} \sum_{i=0}^{N-1} \frac{\|\phi_q(t)\|^{2i}}{i!}\right)^{M-L} d\phi_q(t)\right). \quad (3.43)$$

Using similar change of variables introduced in the previous section and after some

mathematical manipulations, we get

$$P(\mathbf{c} \rightarrow \mathbf{e}) \leq \prod_{t=1}^{l} \frac{M!}{\pi^{NL}(M-L)!L!} \left(\pi^N \prod_{i=1}^{N} \left(1 + \lambda_i(t)\frac{E_s}{4N_0}\right)^{-1} \right)^{L-1} \cdot \left(\frac{\pi^N}{(N!)^{M-L}} \sum_{g_1=1}^{N} \cdots \sum_{g_{N(M-L)}=1}^{N} \frac{k_1! \cdots k_N!.}{\prod_{j=1}^{N} \left(1 + \lambda_j(t)\frac{E_s}{4N_0}\right)^{k_j+1}} \right), \quad (3.44)$$

which is possible to be rewritten as

$$P(\mathbf{c} \rightarrow \mathbf{e}) \leq \prod_{t=1}^{l} \left(\frac{M!}{(M-L)!L!(N!)^{M-L}} \right) \cdot \left(\prod_{i=1}^{N} \left(1 + \lambda_i(t)\frac{E_s}{4N_0}\right)^{-L+1} \sum_{g_1=1}^{N} \cdots \sum_{g_{N(M-L)}=1}^{N} \frac{k_1! \cdots k_N!.}{\prod_{j=1}^{N} \left(1 + \lambda_j(t)\frac{E_s}{4N_0}\right)^{k_j+1}} \right). \quad (3.45)$$

Considering the fact that there is only one nonzero eigenvalue when $t \in \varphi(\mathbf{c}, \mathbf{e})$, we get

$$P(\mathbf{c} \rightarrow \mathbf{e}) \leq \left(\frac{M!}{(M-L)!L!(N!)^{M-L}} \right)^{l} \prod_{t \in \varphi(\mathbf{c},\mathbf{e})} \left(1 + \lambda'(t)\frac{E_s}{4N_0}\right)^{-L+1} \cdot \left(\sum_{g_1=1}^{N} \cdots \sum_{g_{N(M-L)}=1}^{N} \frac{k_1! \cdots k_N!.}{\left(1 + \lambda'(t)\frac{E_s}{4N_0}\right)^{k'+1}} \right). \quad (3.46)$$

Using similar argument that led to (3.25), it is possible to simplify the expression

(3.46) at a relatively large SNR as

$$P(\mathbf{c} \to \mathbf{e}) \leq \left(\frac{M!}{(M-L)!L!\,(N!)^{M-L}}\right)^{l} K^{\mu}(M,N,L) \cdot \left(\prod_{t\in\varphi(\mathbf{c},\mathbf{e})} |\mathbf{c}_t - \mathbf{e}_t|^2\right)^{-L} \left(\frac{E_s}{4N_0}\right)^{-\mu L}, \quad (3.47)$$

where $K(M,N,L) = \sum_{g_1=1}^{N} \cdots \sum_{g_{(M-L)N}=1}^{N} k_1! \cdots k_N!$. By comparing (3.47) and (3.12) it is clear that the diversity order resulting from selecting the best L antennas is reduced from μM to μL. Similar to the $L = 1$ case, since the inequality in (3.47) gives an upper bound on the PEP, we still need to find a lower bound on the PEP to conclude that the diversity order is reduced to μL.

In order to find a lower bound for this case, we use (3.27) and write the conditional PEP when the best L antennas are selected as

$$P(\mathbf{c} \to \mathbf{e} \mid \Phi_1(t), \ldots, \Phi_L(t), t \in \{1,2,\ldots,l\}) = \frac{1}{\pi}\int_0^{\frac{\pi}{2}} e^{\left(-\sum_{t=1}^{l}\sum_{j=1}^{L}\left(\Phi_j(t)C(t)\Phi_j^*(t)\right)\frac{E_s}{8N_0\sin^2\theta}\right)} d\theta. \quad (3.48)$$

To find an expression for the PEP, we average (3.48) with respect to $\Phi_1(t), \ldots, \Phi_L(t)$

as

$$P(\mathbf{c} \rightarrow \mathbf{e}) = \frac{1}{\pi} \int_0^{\frac{\pi}{2}} \prod_{t=1}^{l} \frac{M!}{\pi^{NL}(M-L)!L!L} \sum_{q=1}^{L} \int_{\Phi_L(t)} \cdots \int_{\Phi_1(t)} \cdot e^{\left(-\sum_{j=1}^{L} \left(\Phi_j(t) C(t) \Phi_j^*(t)\right) \frac{E_s}{8N_0 \sin^2\theta} \right)} e^{-\sum_{j=1}^{L} \|\phi_j(t)\|^2} \cdot \left[1 - e^{-\|\phi_q(t)\|^2} \sum_{i=0}^{N-1} \frac{\|\phi_q(t)\|^{2i}}{i!} \right]^{M-L} d\phi_1(t) \cdots d\phi_L(t), \quad (3.49)$$

which after implementing mathematical manipulations similar to what led to (3.45), we obtain

$$P(\mathbf{c} \rightarrow \mathbf{e}) \geqslant \frac{1}{\pi} \int_0^{\frac{\pi}{2}} \prod_{t=1}^{l} \left(\frac{M!}{(N!)^{M-L}(M-L)!L!} \right) \cdot \left(\prod_{i=1}^{N} \left(1 + \lambda_i(t) \frac{E_s}{8N_0 \sin^2\theta} \right)^{-L+1} \right) \cdot \left(\sum_{g_1=1}^{N} \cdots \sum_{g_{(M-1)N}=1}^{N} \frac{k_1! \cdots k_N!}{\prod_{j=1}^{N} \left(M - L + 1 + \lambda_j(t) \frac{E_s}{8N_0 \sin^2\theta} \right)^{k_j+1}} \right) d\theta, \quad (3.50)$$

It is possible to rewrite the expression (3.50) as

$$P(\mathbf{c} \to \mathbf{e}) \geqslant \frac{1}{\pi}\left(\frac{M!}{(N!)^{M-L}(M-L)!L!}\right)^{l} \int_0^{\frac{\pi}{2}} \prod_{t=1}^{l}\left(\prod_{i=1}^{N}\left(1+\lambda_i(t)\frac{E_s}{8N_0\sin^2\theta}\right)^{-L+1}\right) \cdot \left(\sum_{g_1=1}^{N}\cdots\sum_{g_{(M-1)N}=1}^{N} \frac{k_1!\cdots k_N!}{(M-L+1)^{\sum_{j=1}^{N}k_j+1}\prod_{j=1}^{N}\left(1+\lambda_j(t)\frac{E_s}{8(M-L+1)N_0\sin^2\theta}\right)^{k_j+1}}\right) d\theta. \quad (3.51)$$

Using $\sum_{j=1}^{N} k_j = (M-L)N$ and considering the fact that in each time interval there exists maximally one nonzero eigenvalue, we have

$$P(\mathbf{c} \to \mathbf{e}) \geqslant \frac{(M-L+1)^{\mu}}{\pi}\left(\frac{M!}{(N!)^{M-L}(M-L)!L!\,(M-L+1)^{N(M-L+1)}}\right)^{l} \cdot K^{\mu}(M,N,L)\left(\prod_{t\in\varphi(\mathbf{c},\mathbf{e})}|\mathbf{c}_t-\mathbf{e}_t|^2\right)^{-L} \cdot \left(\frac{E_s}{4N_0}\right)^{-\mu L}\int_0^{\frac{\pi}{2}}\left(\frac{1}{2\sin^2\theta}\right)^{-\mu L} d\theta. \quad (3.52)$$

This is a lower bound on the PEP when system selects the best L antennas. From (3.47) and (3.52), we clearly see that the PEP is bounded between two curves that have the same slope on a log-to-log scale, which is μL in this case. Therefore, the diversity order resulting from selecting the best L antennas is reduced from μM to μL. Moreover, the reduction of diversity order from μM to μL means that employing

antenna selection makes the diversity order dependent on the number of selected antennas. To further validate the upper bounds derived above, we now find values for the constants $K(M, N, 1)$ and $K(M, N, L)$ for specific values of N.

Table 3.1: Values of the Constant K(N,M,L) for Specific Values of N.

$K(N, M, L)$	$L = 1$	$L > 1$
$N = 2$	$[2(M-1)]!$	$[2(M-L)]!$
$N = 3$	$[3M-2]!$	$[3(M-L)+1]!$
$N = 4$	$\frac{1}{2}[4M-2]!$	$\frac{1}{2}[4(M-L)+2]!$

3.4 Numerical Examples and Simulation Results

In this section, we illustrate the results of this part of the work by considering two STTC coding examples: the four-phase-shift-keying (4-PSK), 4-state code, and the 8-PSK, 8-state code given in [4]. The number of transmit antennas in all cases considered is $N = 2$. A fast flat fading channel with zero-mean channel coefficients is assumed. The length of a frame coming out of each transmit antenna is $l = 130$. In all cases, where applicable, antenna selection is done based on maximizing the received SNR.

Figs. 3.5 and 3.6 show the trellis diagrams of the 4-PSK, 4-state and 8-PSK 8-state codes, respectively. Tables 3.2 and 3.3 show the output symbol pairs of these trellis diagrams for each state transition [4]. The constellation diagrams of these signals are shown in Fig. 3.7.

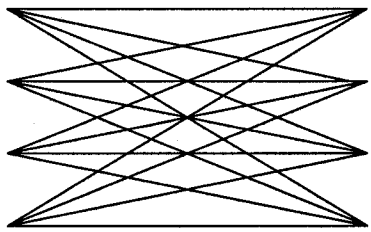

Figure 3.5: 4-PSK, 4-state.

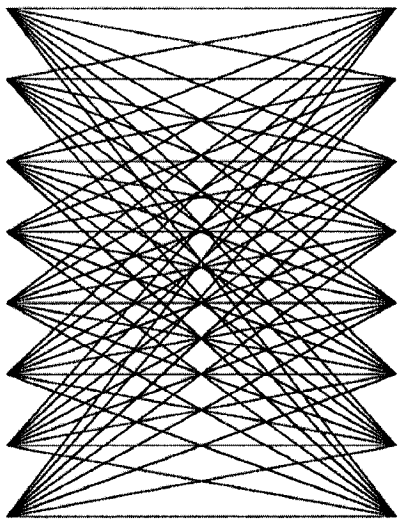

Figure 3.6: 8-PSK, 8-state.

3.4.1 Numerical Results

In this section, we present some numerical examples to validate the upper bounds on the PEP with antenna selection that were derived above. Evaluating the average PEP is possible by averaging (3.2) over a large number of channel realizations while

Table 3.2: Output symbol pairs, 4-PSK.

	0	1	2	3
0	00	01	02	03
1	10	11	12	13
2	20	21	22	23
3	30	31	32	33

Table 3.3: Output symbol pairs, 8-PSK.

	0	1	2	3	4	5	6	7
0	00	01	02	03	04	05	06	07
1	50	51	52	53	54	55	56	57
2	20	21	22	23	24	25	26	27
3	70	71	72	73	74	75	76	77
4	40	41	42	43	44	45	46	47
5	10	11	12	13	14	15	16	17
6	60	61	62	63	64	65	66	67
7	30	31	32	33	34	35	36	37

assuming a particular error event length, and then repeating the averaging over all possible error events of the same length. We consider MIMO systems with two and three receive antennas, and two transmit antennas. The STTC used for the numerical examples is the 4-PSK presented in [4]. We consider error event lengths two and three because they are the ones that dominate the performance at high SNR. The length of an error event is the number of consecutive symbols which have been erroneously decoded.

In Figs. 3.8 and 3.9, examples of length-2 and 3 error events are shown. In these figures, the solid lines show the correct path, while the dotted ones are the incorrect paths. Considering the graph in Figs. 3.8, for each correct path, there exist 3 incorrect paths in the case of length-2 error event. For the situation shown in Fig. 3.9, there

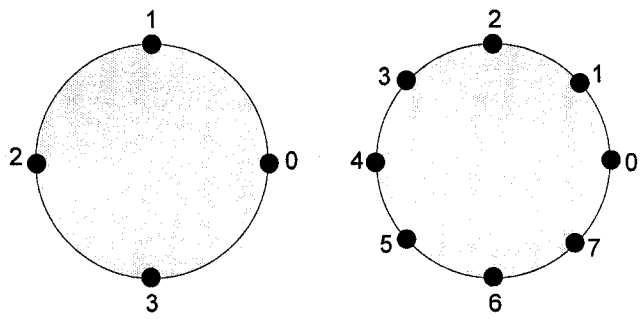

Figure 3.7: Constellation diagrams for 4-PSK (left) and 8-PSK (right) codes.

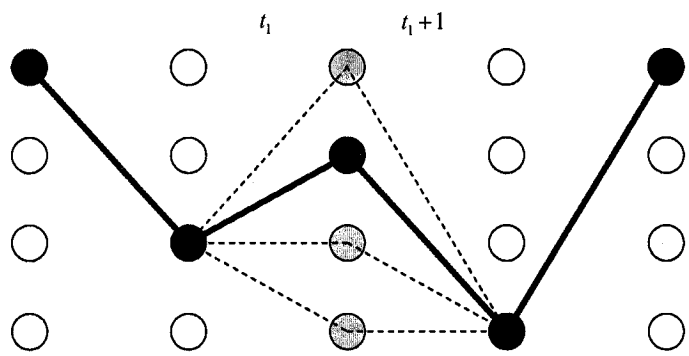

Figure 3.8: length-2 error event.

exist 15 incorrect paths, where we showed only 9 of them which are considered as length-3 error event.

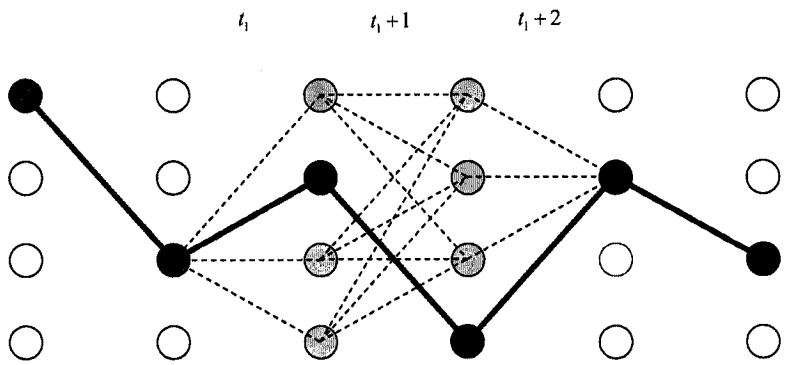

Figure 3.9: length-3 error event.

Assuming only one antenna gets selected at a time, (3.4) can be rewritten as

$$d^2(\mathbf{c},\mathbf{e}) = \sum_{t=1}^{l} \Phi_1(t) C(t) \Phi_1^*(t), \tag{3.53}$$

where $C(t)_{pq} = (c_t^p - e_t^p)\,\overline{(c_t^q - e_t^q)}$ and $\Phi_1(k)$ has the largest norm in time duration t, as defined in (3.13). For the case of selecting more than one antenna, say L, we can rewrite (3.4) as

$$d^2(\mathbf{c},\mathbf{e}) = \sum_{t=1}^{l} \sum_{j=1}^{L} \Phi_j(t) C(t) \Phi_j^*(t), \tag{3.54}$$

where $\Phi_1(k), \ldots, \Phi_L(k)$ are defined in (3.38). Assuming a particular error event

length, evaluating the average PEP is possible by averaging on (3.2) with the help of (3.53) or (3.54) over a large number of channel realizataions, and then repeating the averaging over all possible error sequences of the same length.

Considering the above discussion, we evaluated the average PEP for various selection scenarios, shown in Figs. 3.10 and 3.11. For all cases shown in these figures, the number of transmit antennas is $N = 2$. Moreover, the number of receive antennas for the system corresponding to Fig. 3.10 and 3.11 is $M = 2$ and 3, respectively.

In Fig. 3.10 the results are shown for the case of systems with length-2 and 3 error events with $N = 2$ and $M = 2$. The number of antennas in both of receive and transmit sides are 2. As shown in the figure, the slope of the curves before and after antenna selection, are not the same, which is unlike the case of slow fading channel and in agreement with analytical results.

Moreover, it is possible to compare the slope of the curves for different error event lengths. The curves in this figure show that the diversity order of the antenna selection system, for two different error events of length 2 and 3, and for a fixed number of selected antennas, are the same. Based on the result in Fig. 3.10, and for a system with the fixed number of total available antennas, the diversity order of the antenna selection system is a function of the number of selected antennas.

Fig. 3.11 presents the results for systems with $M = 3$ receive antennas. The error event lengths considered are 2 and 3. As the curves of the figure show, the slope of the curves are different before and after employing antenna selection. This confirms that the diversity order is not preserved with antenna selection.

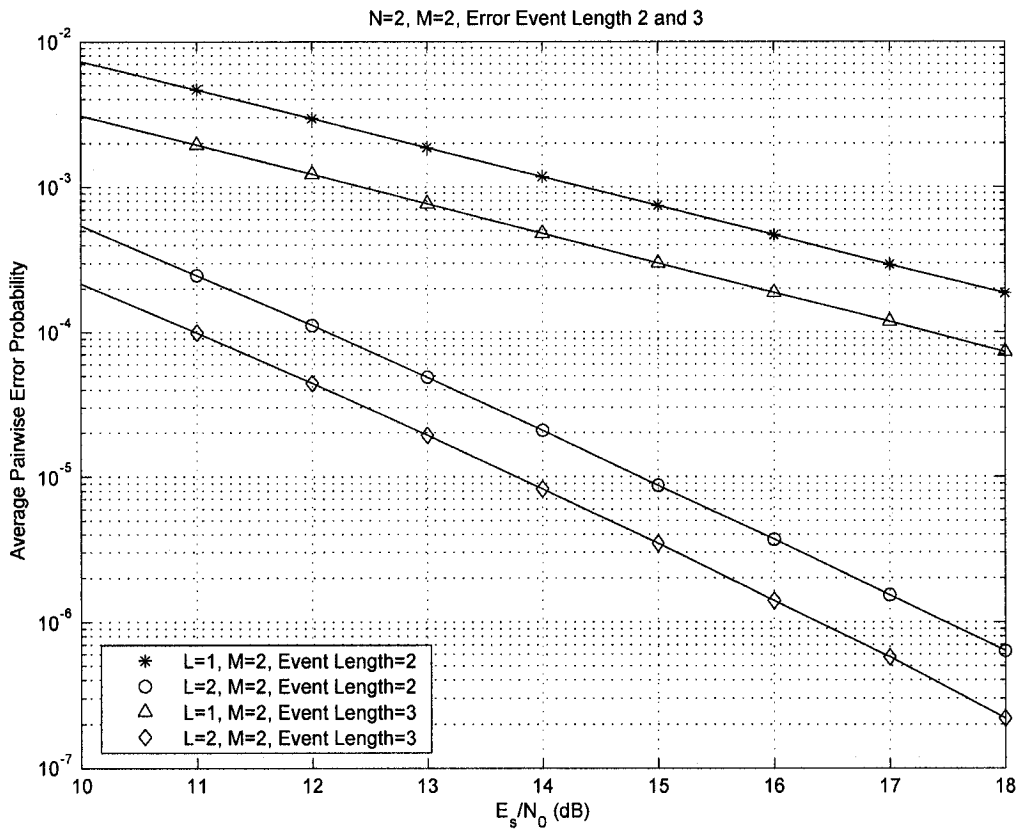

Figure 3.10: Average PEP for $M = 2$ and length-2 and 3 error events.

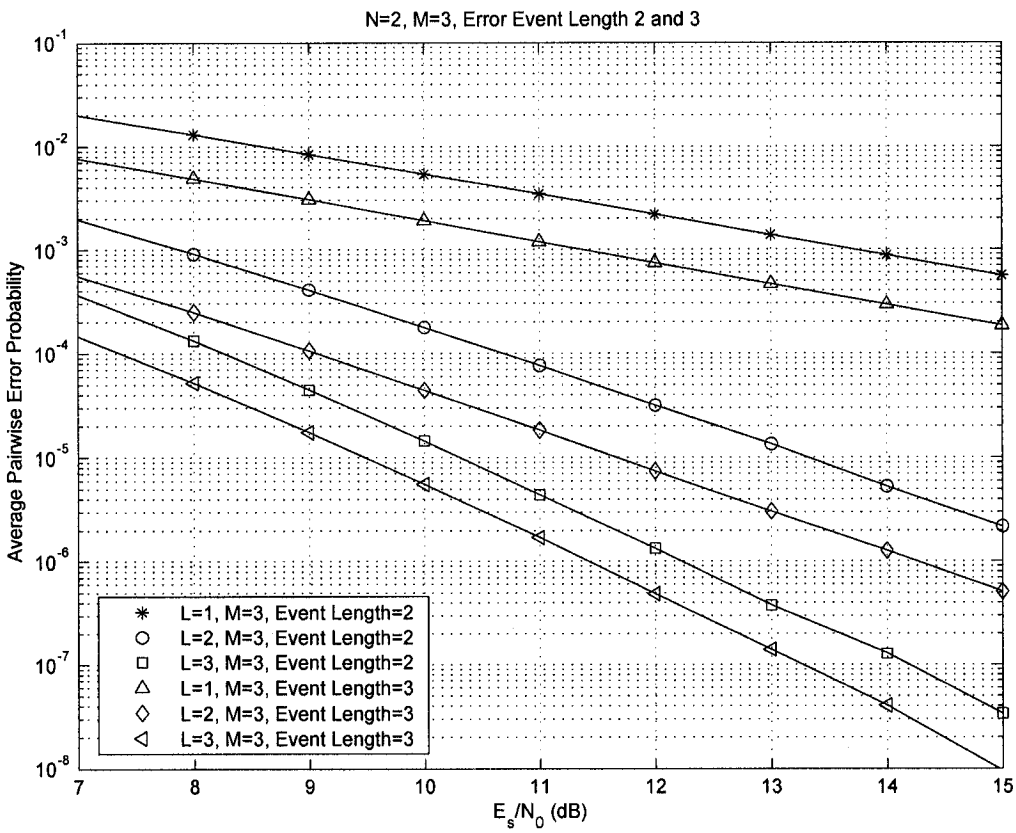

Figure 3.11: Average PEP for $M = 3$ and length-2 and 3 error events.

The results for various selection scenarios and different error event lengths shown in Fig. 3.11 confirm that the diversity order of an antenna selection system is a function of the number of the selected antennas, and not the number of total available antennas. Based on these results, when the number of selected antennas is fixed, the diversity order does not change, regardless of the number of available receive antennas. Therefore, for a fixed number of selected antennas, increasing the number of receive antennas only increases the coding gain of the system.

3.4.2 Simulation Results

In Figs. 3.12 – 3.15, we plot the frame error rate (FER) against the SNR in dB for various cases of antenna selection for the 4-PSK, 4-state and 8-PSK, 8-state codes. We examine the following cases: $M = 3$ with $L = 1, 2, 3$; $M = 2$ with $L = 1, 2$ and $M = 1$ with $L = 1$. The results in Fig. 3.12, which are for a code system of 4-PSK, 4-state, show that the slopes of the performance curves corresponding to a specific L, for all M, are the same, suggesting that their diversity order is the same, which agrees with the analytical results derived in this chapter. However, this additional coding gain becomes smaller as M increases. For instance, at $FER = 10^{-3}$, the case $M = 2$, $L = 1$ achieves a gain of bout 3.0 dB over the case $M = 1$, $L = 1$, whereas only an additional 0.5 dB is achieved in the case $M = 3$, $L = 1$.

In Fig. 3.13, we plot the FER against the SNR in dB for the 8-PSK case for the same antenna selection scenarios considered in Fig. 3.12. It is clear from the figure that the diversity order deteriorates with antenna selection. It is also evident

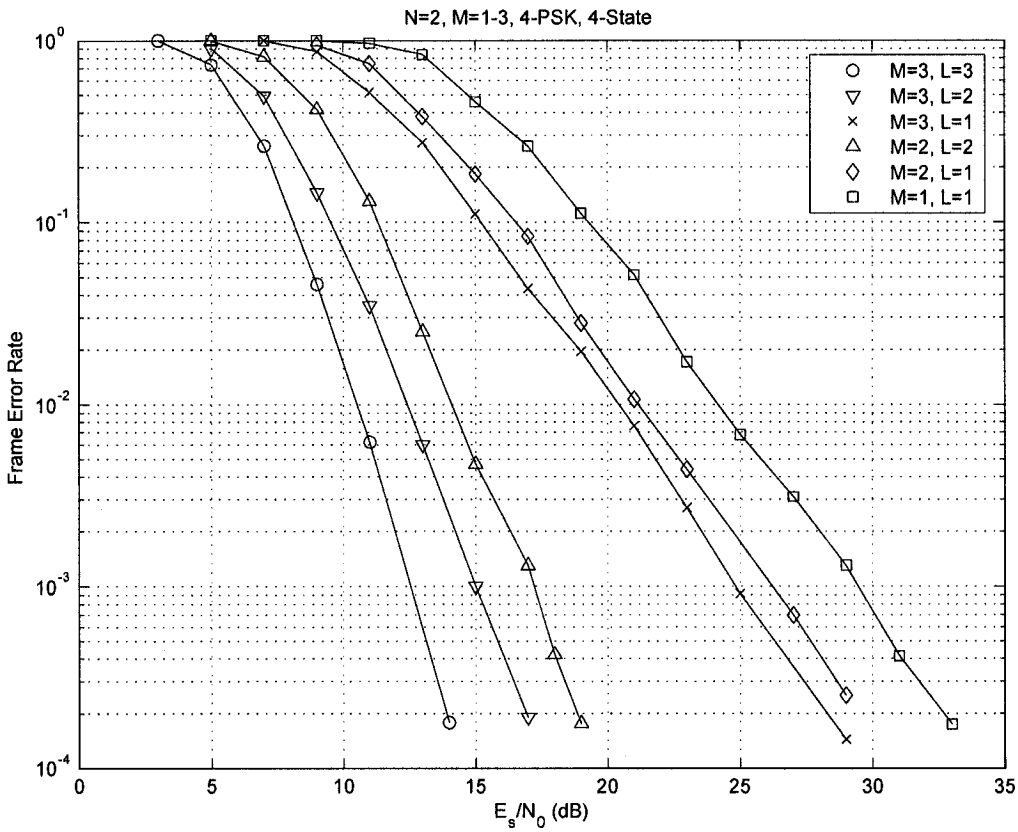

Figure 3.12: FER performance comparison between various antenna selection scenarios in fast fading for 4-PSK, 4-state code.

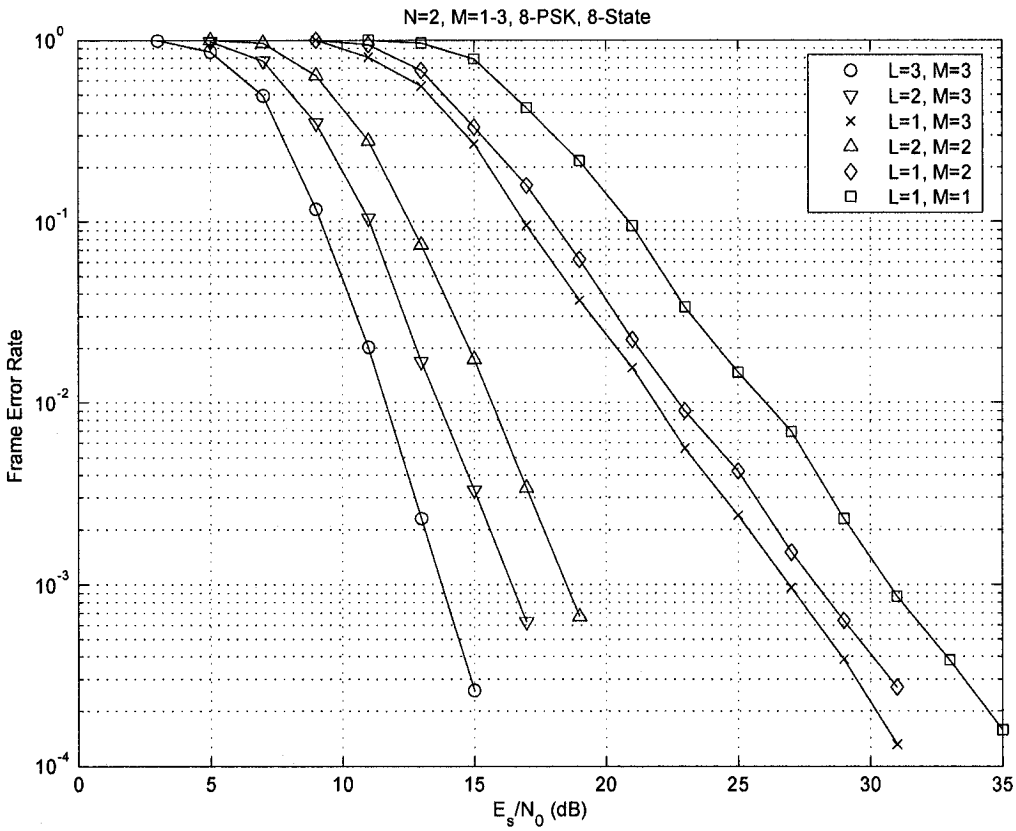

Figure 3.13: FER performance comparison between various antenna selection scenarios in fast fading for 8-PSK, 8-state code.

from the figure that the additional coding gain achieved due to using larger M, while keeping L fixed, becomes marginal as M increases.

Fig. 3.14 shows simulation results for the case $M = 1, 2, 3$ and $L = 1$. The results are for the 4-PSK and 8-PSK cases. From the figure, it is clear that the slopes of the curves are the same, regardless of the number of total available receive antennas. Fig. 3.15 shows the results for the cases $M = 2, 3$ and $L = 2$. This plot also confirms that the diversity order in a fast fading channel depends on the number of selected antennas and not on the total available receive antennas.

For comparison purposes, we include here some simulation results for the quasi-static fading case for the 4-PSK, 4-state space-time code presented in [4]. These results are shown in Fig. 3.16 [21]. The antenna selection scenarios considered here are the same as those considered for fast fading. We observe from the figure that all of the performance curves corresponding to a specific M, for all L, have the same slope, suggesting that antenna diversity is preserved with antenna selection. However, as observed from the figure, the penalty for antenna selection is a reduction in the coding gain, which is expected as well.

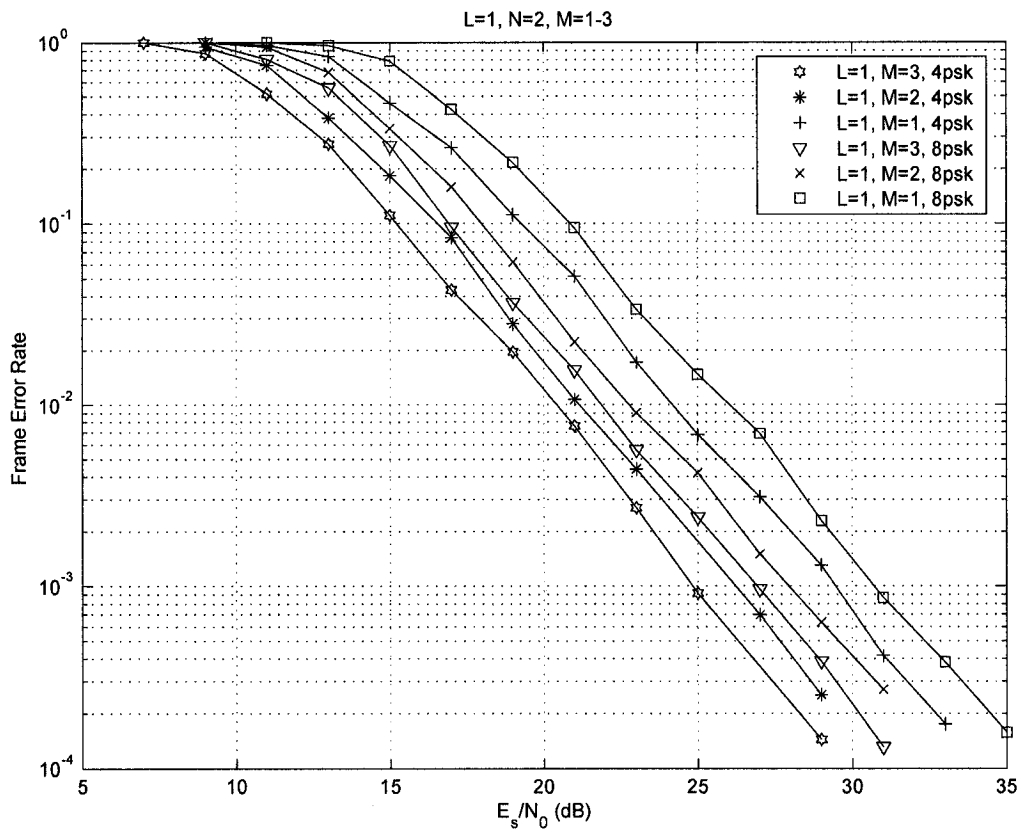

Figure 3.14: FER performance results for $L = 1$ and for the 4-PSK 4-state, 8-PSK 8-state codes.

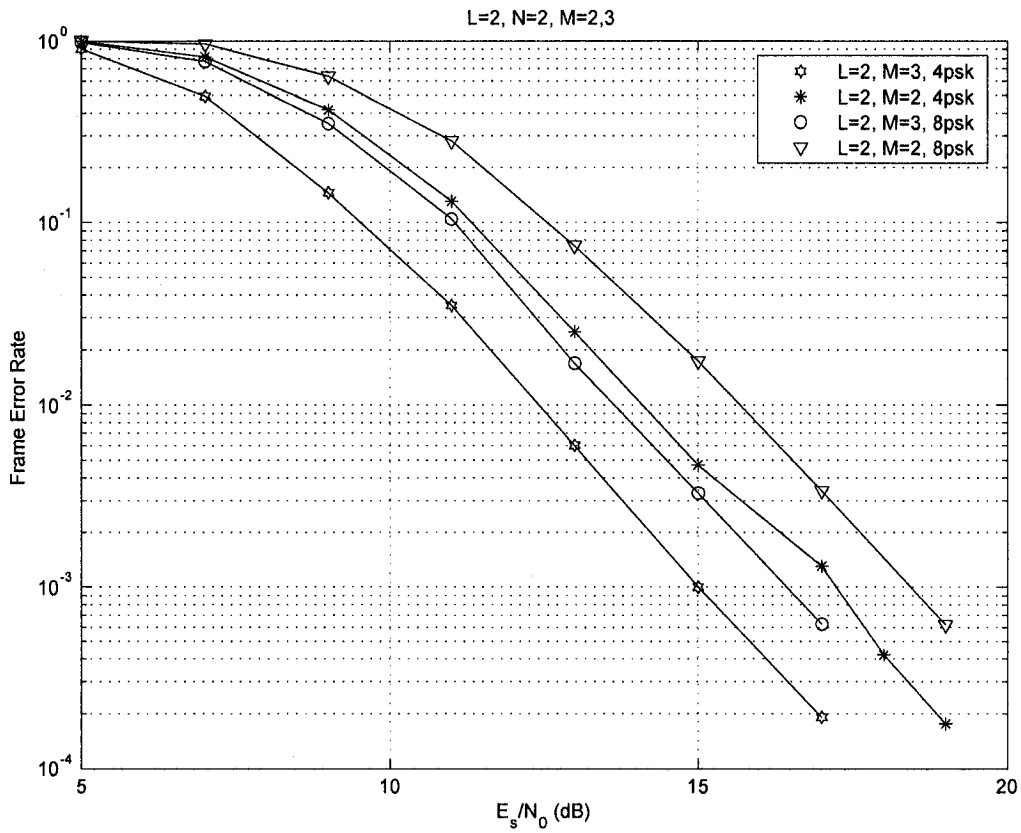

Figure 3.15: FER performance results for $L = 2$ and for the 4-PSK 4-state, 8-PSK 8-state codes.

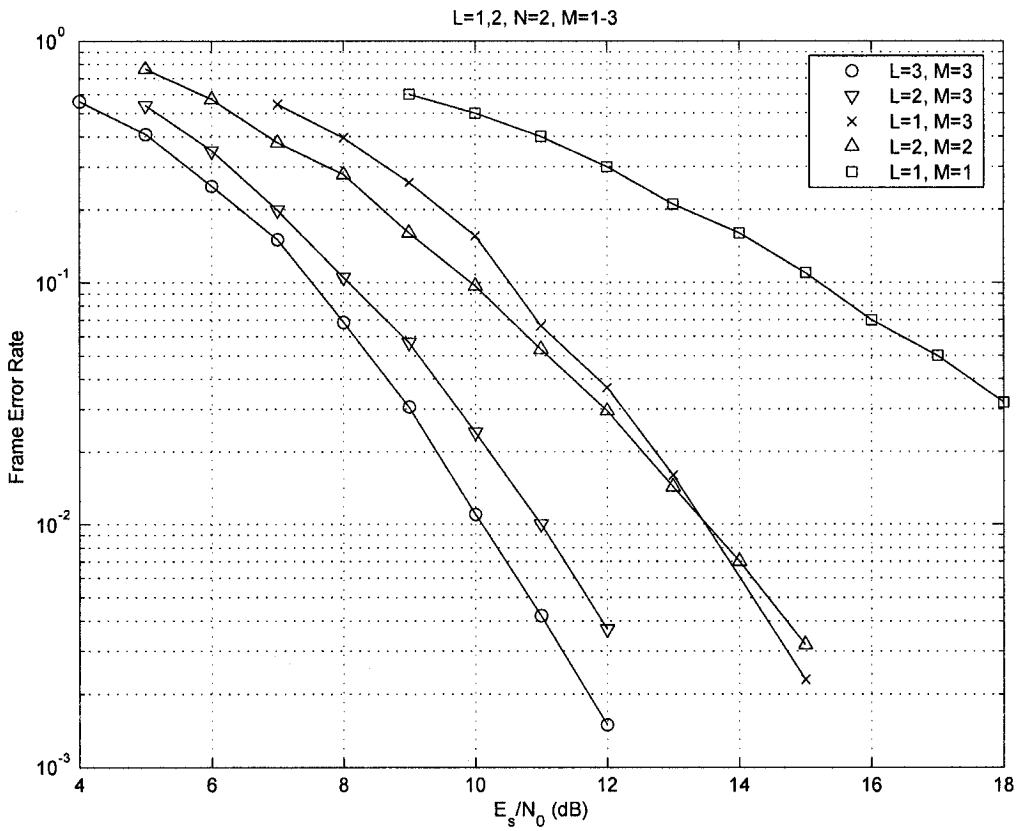

Figure 3.16: FER performance comparison between various antenna selection scenarios in slow fading for 4-PSK, 4-state code [21].

3.5 Conclusion

In this chapter, we have examined the performance of space-time trellis codes over fast fading channels with antenna selection at the receiver. We have adopted a selection criterion that is maximizing the received SNR. We have demonstrated that the diversity order deteriorates with antenna selection, and the resulting diversity order is a linear function of the number of selected antennas. Therefore, adding more receive antennas while keeping the number of selected antennas unchanged does not increase the diversity order. The only effect of doing so is an increase in the coding gain. This result is unlike the case for quasi-static fading where the diversity order is maintained with antenna selection as long as the underlying space-time code is full rank. A thorough mathematical analysis has been developed to understand the phenomenon, which was strongly supported by numerical examples and simulation results.

Chapter 4

Antenna Selection for Block Fading Channels

4.1 Introduction

In this chapter, we consider receive antenna selection for STTCs over block fading channels, where the channel coefficients fade independently from one block of symbols to another. A block is defined to be a set of several consecutive symbols within a data frame. The block fading model is used to model a wide range of practical communication channels because it encompasses a wide range of mobility and data rates. Fast and slow fading channels are two extreme cases of block fading. Therefore, understanding the impact of antenna selection over block fading channels helps understand the results for slow fading ([21], [22]) and fast fading ([?]−[?]) channels .

For a given number of receive antennas M, we assume that the receiver uses

L out of the available M antennas where the selected antennas are those whose instantaneous SNRs are largest. This is achieved by comparing the sums of the magnitude squares of the fading coefficients at each receive antenna and selecting those (L of them) corresponding to the largest sums. We assume that the receiver has full knowledge of the CSI. We derive explicit upper bounds on the pairwise error probability for the above system. We show that the diversity order with antenna selection is dictated by the number of selected antennas and not by the number of the available antennas. This is unlike the case for quasi-static fading channels [21], but is similar to the case of fast fading channel. However, using more antennas results in an improvement in the coding gain due to the increase in the average received SNR after selection. We present several numerical examples that validate the results.

The rest of the chapter is outlined as follows. In Section 4.2, we introduce the system model and some preliminaries. In Section 4.3 we present some results for the full-complexity system. Then, in Section 4.4, we derive explicit upper bounds on the PEP with receive antenna selection. In Section 4.5, we provide numerical examples and simulation results that support our analysis. Finally, we conclude the chapter in Section 4.6.

4.2 System Model

The system under consideration, shown in Fig. 4.1, models a wireless communication system equipped with N antennas at the transmitter and M antennas at

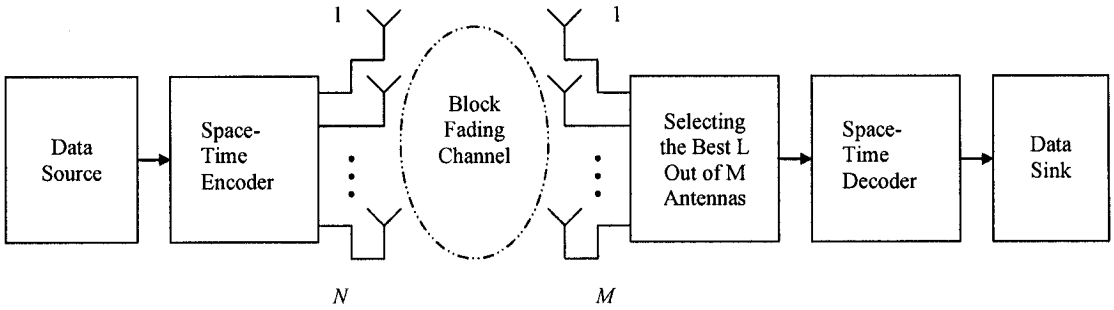

Figure 4.1: System model.

the receiver side. The space-time encoder encodes the data and then feeds it into a serial-to-parallel converter, to provide N parallel streams which are transmitted from N transmit antennas simultaneously. Blocks that involve modulation, demodulation, etc., have been suppressed from the figure due to their irrelevance in the analysis.

At the receiver, after demodulation, matched-filtering, and sampling, the signal r_t^j received by antenna j at time t is given by

$$r_t^j = \sum_{i=1}^{N} \alpha_{i,j}(t) c_t^i + w_t^j, \tag{4.1}$$

where c_t^i is the signal transmitted from antenna i at time t, and the noise terms w_t^j are zero-mean independent complex Gaussian random variables with variance $N_0/2$ per dimension. The coefficients $\alpha_{i,j}(t)$ for $i = 1, 2, \ldots, N$, $j = 1, 2, \ldots, M$, and $t = 1, 2, \ldots, l$ model the fading for the channel between the i^{th} transmit and j^{th} receive antennas at time t, and are assumed to be complex Gaussian random variables. In this study, we assume block flat fading channel, i.e., the fading coefficients $\alpha_{i,j}(t)$

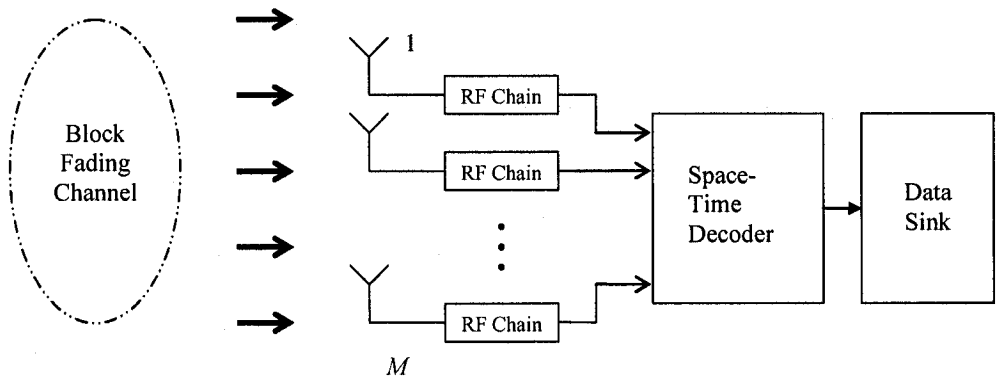

Figure 4.2: Full-complexity system.

change independently from one block of symbols to another. Let l denote the length of the data frame transmitted from each transmit antenna, and let δ denote the length of the faded block, i.e., $1 \leqslant \delta \leqslant l$. Note that when $\delta = l$ the channel becomes quassi-static fading (slow fading), whereas when $\delta = 1$, the channel becomes fast fading. Furthermore, the subchannels are assumed to fade independently.

4.3 Full-Complexity System

4.3.1 Diversity Order

A MIMO system that is using all of the available antennas is referred to as a full-complexity system (see Fig. 4.2). Assuming maximum-likelihood decoding and prefect knowledge of the CSI at the receiver, the conditional PEP that the receiver

decides erroneously on the codeword

$$\mathbf{e} = e_1^1 e_1^2 \cdots e_1^N e_2^1 e_2^2 \cdots e_2^N \cdots e_l^1 e_l^2 \cdots e_l^N,$$

given that the codeword

$$\mathbf{c} = c_1^1 c_1^2 \cdots c_1^N c_2^1 c_2^2 \cdots c_2^N \cdots c_l^1 c_l^2 \cdots c_l^N$$

has been transmitted is upper bounded by

$$P\left(\mathbf{c} \rightarrow \mathbf{e} \,|\, \boldsymbol{\alpha}\right) \leq e^{\left(-d^2(\mathbf{c},\mathbf{e})E_s/4N_0\right)}, \tag{4.2}$$

where $\boldsymbol{\alpha} = \{\alpha_{i,j}(t) : 1 \leq i \leq N,\ 1 \leq j \leq M,\ 1 \leq t \leq l\}$ and

$$d^2\left(\mathbf{c},\mathbf{e}\right) = \sum_{t=1}^{l} \sum_{j=1}^{M} \left| \sum_{i=1}^{N} \alpha_{i,j}(t) \left(c_t^i - e_t^i\right) \right|^2. \tag{4.3}$$

After some simple manipulations, (4.3) can be rewritten as

$$d^2\left(\mathbf{c},\mathbf{e}\right) = \sum_{t=1}^{l} \sum_{j=1}^{M} \Psi_j(t) C(t) \Psi_j^*(t), \tag{4.4}$$

where $\Psi_j(t) = (\alpha_{1,j}(t), \ldots, \alpha_{N,j}(t))$ and $C(t)$ is a matrix whose $(pq)^{th}$ entry is $C(t)_{pq} = (c_t^p - e_t^p)\,\overline{(c_t^q - e_t^q)}$ for $p, q = 1, \ldots, N$. Without loss of generality, let us assume that each frame (of length l) consists of K blocks, each of length δ, i.e.,

$l = K\delta$. As such, (4.4) can be rewritten as

$$d^2(\mathbf{c},\mathbf{e}) = \sum_{j=1}^{M}(\sum_{t=1}^{\delta}\Psi_j(t)C(t)\Psi_j^*(t) + \sum_{t=\delta+1}^{2\delta}\Psi_j(t)C(t)\Psi_j^*(t) + \cdots + \sum_{t=(K-1)\delta+1}^{K\delta}\Psi_j(t)C(t)\Psi_j^*(t)). \quad (4.5)$$

Since the elements of $\Psi_j(t)$ are fixed in a block, we can rewrite (4.5) as

$$d^2(\mathbf{c},\mathbf{e}) = \sum_{j=1}^{M}\Psi_j(1)\left(\sum_{t=1}^{\delta}C(t)\right)\Psi_j^*(1) + \Psi_j(\delta+1)\left(\sum_{t=\delta+1}^{2\delta}C(t)\right)\Psi_j^*(\delta+1) + \cdots + \Psi_j((K-1)\,\delta+1)\left(\sum_{t=(K-1)\delta+1}^{K\delta}C(t)\right)\Psi_j^*((K-1)\,\delta+1). \quad (4.6)$$

By defining

$$A(k) \triangleq \sum_{t=(k-1)\delta+1}^{k\delta}C(t), \quad (4.7)$$

and using the change of variable $\Omega_j(k) = \Psi_j((k-1)\,\delta+1)$, we can express (4.6) as

$$d^2(\mathbf{c},\mathbf{e}) = \sum_{k=1}^{K}\sum_{j=1}^{M}\Omega_j(k)A(k)\Omega_j^*(k). \quad (4.8)$$

Since the matrix $A(k)$ is Hermitian, there exists a unitary matrix $V(k)$ such that $D(k) = V(k)A(k)V^*(k)$, where $D(k)$ is a real diagonal matrix with eigenvalues $\lambda_i(k)$ for $i = 1,\ldots,N$. The rows of $V(k)$ are a complete orthonormal basis of $\mathbb{C}^{\mathbb{N}}$ given by eigenvectors of $A(k)$. Moreover, the diagonal elements of $D(k)$ are the eigenvalues of

$A(k)$. Now let $(\beta_{1,j}(k), \beta_{2,j}(k), \ldots, \beta_{N,j}(k)) = \Omega_j(k)V^*(k)$. Considering the fact that the fading coefficients are complex Gaussian random variables with zero mean and variance 0.5 per dimension, the coefficients $\beta_{i,j}(k)$, for $1 \leq i \leq N$, $1 \leq j \leq M$, $1 \leq k \leq K$, are independent complex Gaussian random variables with zero mean and variance 0.5 per dimension [4]. As such, (4.8) can be re-written as

$$d^2(\mathbf{c}, \mathbf{e}) = \sum_{k=1}^{K} \sum_{j=1}^{M} \sum_{i=1}^{N} |\beta_{i,j}(k)|^2 \lambda_i(k), \tag{4.9}$$

where $|\beta_{i,j}(k)|$ are Rayleigh distributed random variables. Averaging (4.2) with respect to the random variables $|\beta_{i,j}(t)|$ yields

$$P(\mathbf{c} \rightarrow \mathbf{e}) \leq \prod_{k=1}^{K} \prod_{j=1}^{M} \prod_{i=1}^{N} \int_{0}^{\infty} 2 |\beta_{i,j}(k)| e^{\left(-|\beta_{i,j}(k)|^2\right)} e^{\left(-\frac{E_s}{4N_0}|\beta_{i,j}(k)|^2 \lambda_i(k)\right)} d|\beta_{i,j}(k)|, \tag{4.10}$$

which can be expressed in a compact form as

$$P(\mathbf{c} \rightarrow \mathbf{e}) \leq \prod_{k=1}^{K} \left(\prod_{i=1}^{r(k)} \left(\frac{1}{1 + \lambda_i(k)\frac{E_s}{4N_0}} \right)^M \right), \tag{4.11}$$

where $r(k)$ denotes the rank of $A(k)$. To simplify the above expression further, let $\psi(\mathbf{c}, \mathbf{e})$ denote the set of block indices over which an error event extends. As such,

when SNR is sufficiently large, (4.11) can be expressed as

$$P(\mathbf{c} \rightarrow \mathbf{e}) \leq \left(\prod_{k \in \psi(\mathbf{c},\mathbf{e})} \left(\prod_{i=1}^{r(k)} \lambda_i(k) \right)^{-M} \right) \left(\frac{E_s}{4N_0} \right)^{-M \sum_{k \in \psi(\mathbf{c},\mathbf{e})} r(k)}, \tag{4.12}$$

which is an upper bound on the PEP for the full-complexity system over block fading.

Note that setting $K = 1$ or $K = l$ converts (4.12) to the PEP upper bound of the full-complexity system over slow and fast fading channels, respectively, suggested by Tarokh, *et al.* in [4]. For example, for the slow fading case, there exists only one block in a frame and as a result, we have only one value for $r(k)$ for a frame, which can be written as $r(k) = r$. Therefore, we have $\sum_{k \in \psi(\mathbf{c},\mathbf{e})} r(k) = r$, and (4.12) converts to

$$P(\mathbf{c} \rightarrow \mathbf{e}) \leq \left(\prod_{i=1}^{r} \lambda_i \right)^{-M} \left(\frac{E_s}{4N_0} \right)^{-rM}, \tag{4.13}$$

which is an upper bound for the slow fading case as shown in [4].

On the other hand, for fast fading case ($K = l$), the length of the block is 1. By defining $\varphi(\mathbf{c}, \mathbf{e})$ and $\mu = |\varphi(\mathbf{c}, \mathbf{e})|$ as the set of time instances $1 \leq t \leq l$ such that $|\mathbf{c}_t - \mathbf{e}_t| \neq 0$ and the size of $\varphi(\mathbf{c}, \mathbf{e})$, respectively, expression (4.12) converts to the bound for fast fading, which is

$$P(\mathbf{c} \rightarrow \mathbf{e}) \leq \left(\prod_{t \in \varphi(\mathbf{c},\mathbf{e})} |\mathbf{c}_t - \mathbf{e}_t|^2 \right)^{-M} \left(\frac{E_s}{4N_0} \right)^{-\mu M}. \tag{4.14}$$

We note that in the above analysis, it is assumed that the length of the block is greater than the number of transmitters, i.e., $\delta \geq N$, which is a reasonable assumption. It is easy to show that for the rank deficient system, the upper bound on the PEP for both cases of $\delta \geq N$ and $\delta < N$ are the same. However, it is possible to show that the diversity order of the full rank system with $\delta \geq N$ and $\delta < N$, are ηMN and $\eta \delta M$, respectively, where $\eta = |\psi(\mathbf{c}, \mathbf{e})|$ denotes the size of $\psi(\mathbf{c}, \mathbf{e})$.

4.3.2 Rank Of $A(k)$

Considering the structure of the $A(k)$, it is important to note that the rank of $A(k)$ depends on the location of the error events in a frame. This has a key role in our mathematical analysis in the next section. In the following we give some examples to explain this phenomenon. In these examples we consider a system with two transmit and two receive antennas.

Example 1 *Length-2 Error Event*

In the first example, we consider the case of error events of length-2. In Figs. 4.3 and 4.4, two different cases of the length-2 error events are shown. Based on (4.7) the general form of $A(k)$ for a length-2 error event that starts at the arbitrary time t_1, occurring in one block (Fig. 4.3), is written as

$$A(k) = \begin{bmatrix} \left|c^1_{t_1+1} - e^1_{t_1+1}\right|^2 & 0 \\ 0 & \left|c^2_{t_1} - e^2_{t_1}\right|^2 \end{bmatrix}, \tag{4.15}$$

which is a full rank matrix.

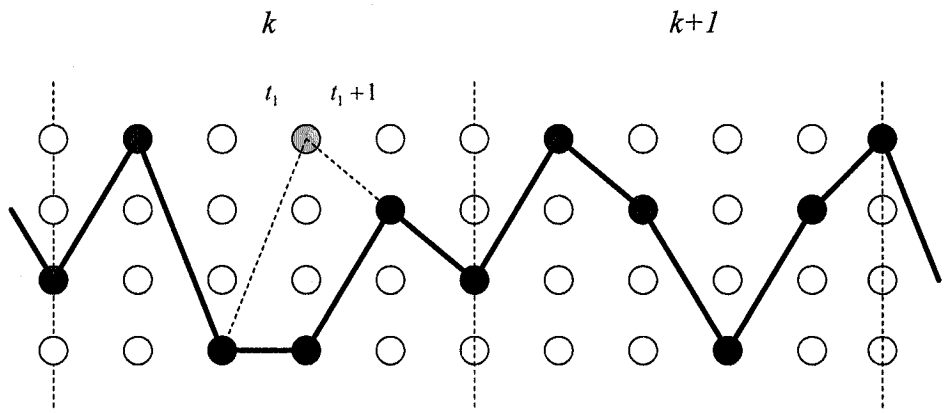

Figure 4.3: Length-2 error event, occurring within one block.

On the other hand, if this length-2 error event starts in one block and ends in the next block (see Fig. 4.4), the general form of the block matrices for this case are written as

$$A(k) = \begin{bmatrix} 0 & 0 \\ 0 & \left|c_{t_1}^2 - e_{t_1}^2\right|^2 \end{bmatrix}, \tag{4.16}$$

and

$$A(k+1) = \begin{bmatrix} \left|c_{t_1+1}^1 - e_{t_1+1}^1\right|^2 & 0 \\ 0 & 0 \end{bmatrix}. \tag{4.17}$$

Consequently, both block matrices are rank deficient.

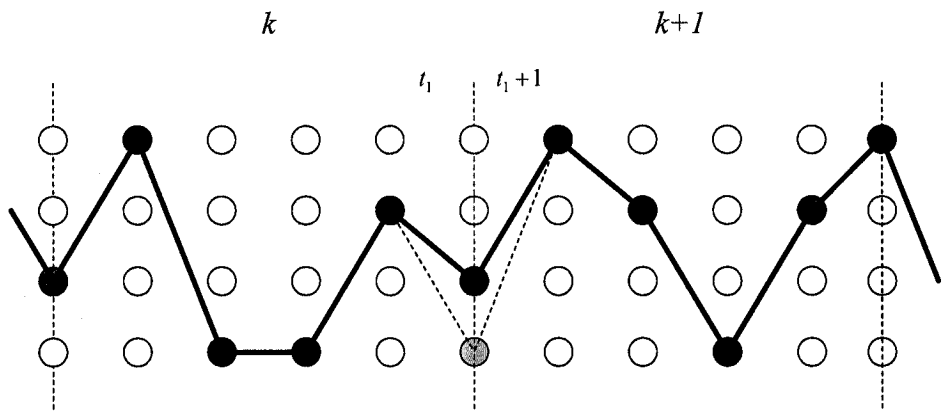

Figure 4.4: Length-2 error event, extending over two consecutive blocks.

Example 2 *Length-3 Error Event*

Now, let us consider error events length-3, that start at $t_1$and extend to $t_1 + 2$. Fig. 4.5 shows an error event of length-3 occurring within the same block. As such, the corresponding codeword difference matrix can be written as

$$A(k) = \begin{bmatrix} \left|c^1_{t_1+1} - e^1_{t_1+1}\right|^2 + \left|c^1_{t_1+2} - e^1_{t_1+2}\right|^2 & \left(c^1_{t_1+1} - e^1_{t_1+1}\right)\overline{\left(c^2_{t_1+1} - e^2_{t_1+1}\right)} \\ \overline{\left(c^1_{t_1+1} - e^1_{t_1+1}\right)}\left(c^2_{t_1+1} - e^2_{t_1+1}\right) & \left|c^2_{t_1} - e^2_{t_1}\right|^2 + \left|c^2_{t_1+1} - e^2_{t_1+1}\right|^2 \end{bmatrix}, \tag{4.18}$$

which is a full rank matrix.

In Fig. 4.6, the error event starts in block k and extends to block $k + 1$. The corresponding codeword difference matrices will be

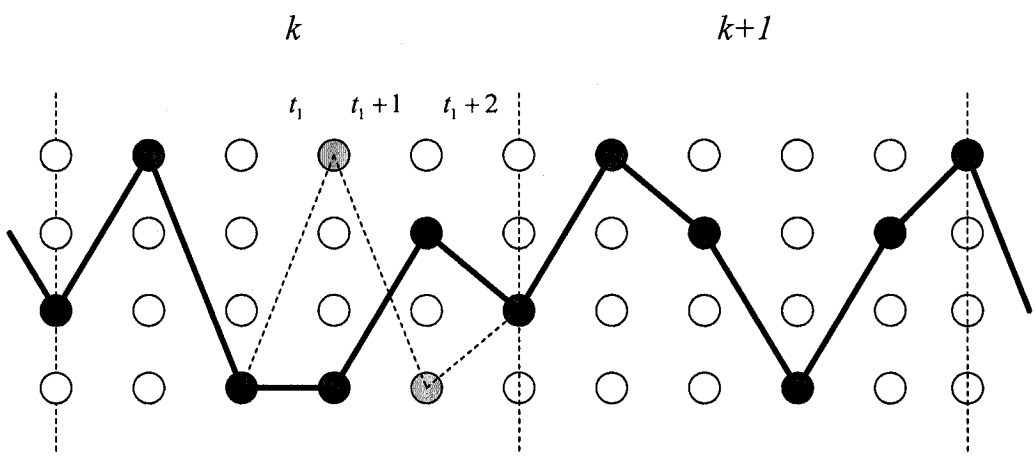

Figure 4.5: Length-3 error event, occurring within one block.

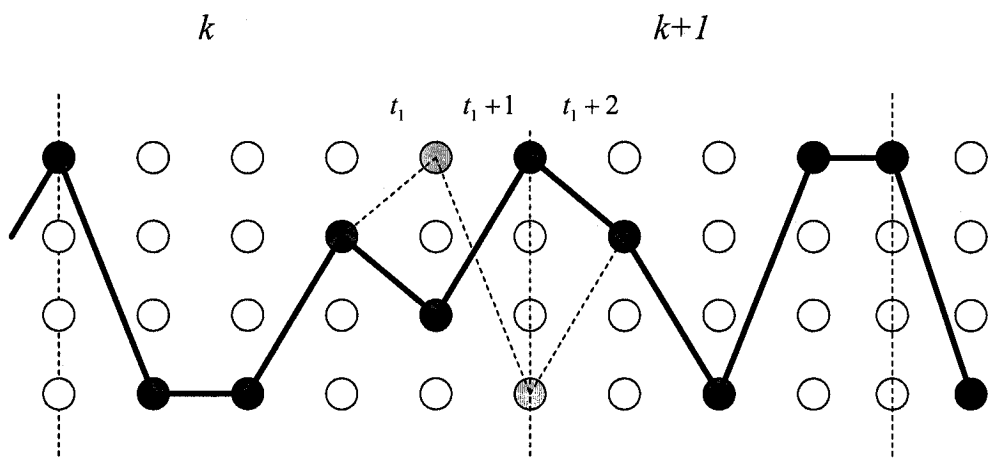

Figure 4.6: Length-3 error event, extending over two consecutive blocks.

$$A(k) = \begin{bmatrix} \left|c^1_{t_1+1} - e^1_{t_1+1}\right|^2 & \left(c^1_{t_1+1} - e^1_{t_1+1}\right)\overline{\left(c^2_{t_1+1} - e^2_{t_1+1}\right)} \\ \overline{\left(c^1_{t_1+1} - e^1_{t_1+1}\right)}\left(c^2_{t_1+1} - e^2_{t_1+1}\right) & \left|c^2_{t_1} - e^2_{t_1}\right|^2 + \left|c^2_{t_1+1} - e^2_{t_1+1}\right|^2 \end{bmatrix}, \tag{4.19}$$

and

$$A(k+1) = \begin{bmatrix} \left|c^1_{t_1+2} - e^1_{t_1+2}\right|^2 & 0 \\ 0 & 0 \end{bmatrix}. \tag{4.20}$$

It is clear that $A(k)$ is full rank, whereas $A(k+1)$ is rank deficient. Therefore, for any error event that starts in a block and ends in a different block, some of the corresponding block matrices are likely to be rank deficient. Since error occurs randomly, there is no guarantee that the block matrices are all full rank. Thus, in the following analysis, we consider the worst case scenario, that is, some of the block matrices are rank deficient.

4.4 Antenna Selection System

In this section, we derive upper bounds on the PEP with antenna selection at the receiver. That is, the case when the receiver uses only L out of the available M receive antennas, where $1 \leq L \leq M$. Note that there are $\binom{M}{L}$ subsets to choose from, but we assume that the selected subset is the one that results in the maximum instantaneous SNR at the receiver. We first derive upper bounds for the case $L = 1$,

i.e., when the receiver selects the best antenna.

4.4.1 Selecting the Best Receive Antenna ($L = 1$)

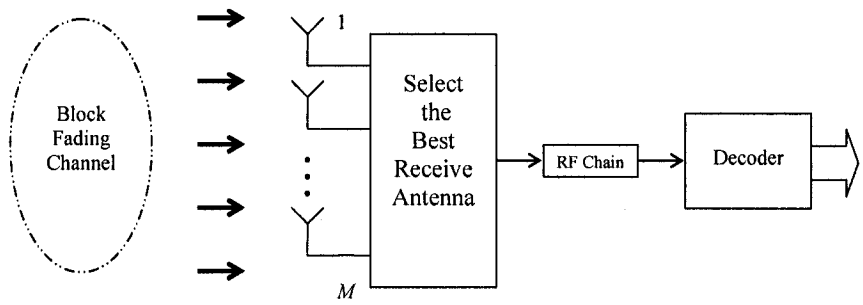

Figure 4.7: Antenna selection system, selecting the best antenna.

Fig. 4.7 shows the model of the antenna selection system that selects the best antenna. The amount of energy picked up by the j^{th} antenna during block k can be represented by $Y_j(k) = \|\Omega_j(k)\|^2$, $j = 1, 2, \ldots, M$, where $\|\cdot\|^2$ denotes the squared norm operator. At the beginning of each block k, the receiver selects the antenna which has the largest term of this $Y_j(k)$ sequence. In order to simplify the analysis we introduce another sequence of M auxiliary random variables such that $X_1(k) \geq X_2(k) \geq \cdots \geq X_M(k)$ which is obtained by rearranging the random sequence $Y_1(k), Y_2(k), \ldots, Y_M(k)$ in an increasing order of magnitude. Furthermore, we represent the random sequence $\Phi_1(k), \ldots, \Phi_M(k)$ as the ordered sequence of $\Omega_1(k), \ldots, \Omega_M(k)$. It is clear that $X_j(k) = \|\Phi_j(k)\|^2$ for $j = 1, 2, \ldots, M$. When the best antenna is selected, the

conditional PEP can be expressed as

$$P\left(\mathbf{c} \rightarrow \mathbf{e} \mid \Phi_1(k), k \in \{1, 2, \ldots, K\}\right) \leq e^{\left(-\sum_{k=1}^{K}\left(\Phi_1(k)A(k)\Phi_1^*(k)\right)\frac{E_s}{4N_0}\right)}, \tag{4.21}$$

where $\Phi_1(k)$ is the vector of N complex Gaussian random variables, corresponding to the receive antenna with the largest instantaneous SNR for the k^{th} block, which are independent and identically distributed (iid). To find the average PEP, we average (4.21) with respect to the distribution of $\Phi_1(k)$. That is,

$$P\left(\mathbf{c} \rightarrow \mathbf{e}\right) \leq \prod_{k=1}^{K} \int_{\mathbb{C}^N} e^{-\left(\Phi_1(k)A(k)\Phi_1^*(k)\right)\frac{E_s}{4N_0}} f_{\Phi_1(k)}\left(\phi_1(k)\right) d\phi_1(k), \tag{4.22}$$

where $\mathbb{C}^N$ denotes the $N-$dimensional complex space and $f_{\Phi_1(k)}\left(\phi_1(k)\right)$ is the pdf of $\Phi_1(k)$ given by [45]

$$f_{\Phi_1(k)}\left(\phi_1(k)\right) = \frac{M}{\pi^N}\left(1 - e^{-\|\phi_1(k)\|^2}\sum_{i=0}^{N-1}\frac{\|\phi_1(k)\|^{2i}}{i!}\right)^{M-1} e^{-\|\phi_1(k)\|^2}. \tag{4.23}$$

By substituting (4.23) into (4.22), using the singular value decomposition of $D(k) = V^*(k)A(k)V(k)$, and applying the change of variables $\mathbf{r}(k) = \Phi_1(k)V(k) =$

$[r_1(k), \ldots, r_N(k)]$ and $r_i(t) = \rho_i(t)e^{j\theta_i(t)}$, we obtain

$$P(\mathbf{c} \rightarrow \mathbf{e}) \leq \prod_{k=1}^{K} M 2^N \int_0^\infty \int_0^\infty \cdots \int_0^\infty e^{\left(-\frac{E_s}{4N_0}\sum_{i=1}^{N}\rho_i^2(k)\lambda_{ii}(k)\right)} \cdot e^{-\sum_{i=1}^{N}\rho_i^2(k)} \left(1 - e^{-\sum_{i=1}^{N}\rho_i^2(k)} \sum_{i=0}^{N-1} \frac{\left(\sum_{i=1}^{N}\rho_i^2(k)\right)^i}{i!}\right)^{M-1} \cdot \left(\prod_{i=1}^{N}\rho_i(k)\right) d\rho_1(k)d\rho_2(k)\cdots d\rho_N(k). \quad (4.24)$$

To simplify the evaluation of the upper bound in (4.24), we note that if $g(v) = 1 - e^{-v}\sum_{i=0}^{N-1}\frac{v^i}{i!}$, then $g(v) \leq \frac{v^N}{N!}$ for $v > 0$ [11]. With the help of this result, defining $v = \sum_{i=1}^{N}\rho_i^2(t)$ and applying the change of variable $u_i(t) = \rho_i^2(t)$, we can rewrite (4.24) as

$$P(\mathbf{c} \rightarrow \mathbf{e}) \leq \prod_{k=1}^{K} \frac{M}{(N!)^{M-1}} \int_0^\infty \cdots \int_0^\infty e^{\left(-\sum_{i=1}^{N}u_i(k)\left[\lambda_{ii}(k)\frac{E_s}{4N_0}+1\right]\right)} \cdot \left(\sum_{i=1}^{N}u_i(k)\right)^{(M-1)N} du_1(k)\cdots du_N(k). \quad (4.25)$$

Carrying out the integration in (4.25) with the assumption that each $A(k)$ for

$k = 1, \cdots, K$ has $r(k)$ non-zero eigenvalues, yields

$$P(\mathbf{c} \to \mathbf{e}) \leq \prod_{k=1}^{K} \frac{M}{(N!)^{M-1}} \sum_{i_1=1}^{N} \cdots \sum_{i_{(M-1)N}=1}^{N} \frac{q_1! q_2! \cdots q_N!}{\left(1 + \lambda_1(k)\frac{E_s}{4N_0}\right)^{q_1'+1} \left(1 + \lambda_2(k)\frac{E_s}{4N_0}\right)^{q_2'+1} \cdots \left(1 + \lambda_{r(k)}(k)\frac{E_s}{4N_0}\right)^{q_{r(k)}'+1}}, \quad (4.26)$$

where $q_i,\ i = 1, \ldots, N$ represents the number of times the term $u_j(k)$ appears in the product

$$u_{i_1}(k) u_{i_2}(k) \cdots u_{i_{(M-1)N}}(k)$$

and $q_i',\ i = 1, \ldots, r(k)$ denotes those values of q_i that appear in the denominator. For a sufficiently large SNR, (4.26) can be written as

$$P(\mathbf{c} \to \mathbf{e}) \leq \left(\frac{M}{(N!)^{M-1}}\right)^{K} \cdot \prod_{k \in \psi(\mathbf{c},\mathbf{e})} \left(\sum_{i_1=1}^{N} \cdots \sum_{i_{(M-1)N}=1}^{N} \frac{\prod_{i=1}^{N} q_i!}{\prod_{j=1}^{r(k)} \lambda_j^{q_j'+1}(k)} \left(\frac{E_s}{4N_0}\right)^{-\sum_{j=1}^{r(k)} q_j'} \right) \cdot \prod_{k \notin \psi(\mathbf{c},\mathbf{e})} \left(\prod_{i=1}^{N} q_i!\right) \left(\frac{E_s}{4N_0}\right)^{-\sum_{k \in \psi(\mathbf{c},\mathbf{e})} r(k)}. \quad (4.27)$$

Considering the expansion of $\left(\sum_{i=1}^{N} u_i(k)\right)^{(M-1)N}$ in (4.25), it is clear that $\sum_{i=1}^{r(k)} q_i' \leq$

$\sum_{i=1}^{N} q_i = (M-1)N$ and we can easily show that

$$P(\mathbf{c} \to \mathbf{e}) \leq \left(\frac{M}{(N!)^{M-1}}\right)^K \cdot \prod_{k \in \psi(\mathbf{c},\mathbf{e})} \left(\prod_{j=1}^{r(k)} \lambda_j^{-1}(k) \sum_{z=0}^{(M-1)N} \sigma_1(k,z) \left(\frac{E_s}{4N_0}\right)^{-z} \right) \cdot \prod_{k \notin \psi(\mathbf{c},\mathbf{e})} \left(\prod_{i=1}^{N} q_i! \right) \left(\frac{E_s}{4N_0}\right)^{-\sum_{k \in \psi(\mathbf{c},\mathbf{e})} r(k)}, \quad (4.28)$$

where $z = \sum_{j=1}^{r(k)} q_j'$, and $\sigma_1(k,z)$ is the summation of the multiplicators of the same exponent terms of SNR. For a sufficiently high SNR (4.28) can be simplified as

$$P(\mathbf{c} \to \mathbf{e}) \leq \left(\frac{M}{(N!)^{M-1}}\right)^K \prod_{k \notin \psi(\mathbf{c},\mathbf{e})} \left(\prod_{i=1}^{N} q_i! \right) \cdot \prod_{k \in \psi(\mathbf{c},\mathbf{e})} \left(\left(\prod_{j=1}^{r(k)} \lambda_j^{-1}(k) \right) \sigma_1(k,0) \right) \left(\frac{E_s}{4N_0}\right)^{-\sum_{k \in \psi(\mathbf{c},\mathbf{e})} r(k)}. \quad (4.29)$$

The upper bound on the PEP given by (4.29) shows that, in a block fading channel, the diversity order when the receiver selects the best antenna is $\sum_{k \in \psi(\mathbf{c},\mathbf{e})} r(k)$. This result is different from the diversity degree of a full-complexity system which is $M \sum_{k \in \psi(\mathbf{c},\mathbf{e})} r(k)$, given by (4.12). However, considering the fact that (4.29) gives an upper bound on the PEP, we need to find a lower bound on the PEP to conclude that the diversity order indeed deteriorates as suggested by (4.29). In order to find this lower bound, we use (3.27) to evaluate the conditional PEP when the best antenna

is selected as

$$P(\mathbf{c} \rightarrow \mathbf{e} \mid \Phi_1(k), k \in \{1, 2, \ldots, K\}) = \frac{1}{\pi} \int_0^{\frac{\pi}{2}} \prod_{k=1}^{K} e^{\left(-\left(\Phi_1(k) A(k) \Phi_1^*(k)\right) \frac{E_s}{8N_0 \sin^2\theta}\right)} d\theta. \quad (4.30)$$

Averaging (4.30) with respect to $\Phi_1(k)$ and repeating steps similar to what lead to (4.24) gives

$$P(\mathbf{c} \rightarrow \mathbf{e}) = \frac{1}{\pi} \int_0^{\frac{\pi}{2}} \prod_{k=1}^{K} M 2^N \int_0^{\infty} \cdots \int_0^{\infty} e^{\left(-\frac{E_s}{8N_0 \sin^2\theta} \left(\sum_{i=1}^{N} \rho_i^2(k) \lambda_{ii}(k)\right)\right)} \cdot \left(1 - e^{-\sum_{i=1}^{N} \rho_i^2(k)} \sum_{i=0}^{N-1} \frac{\left(\sum_{i=1}^{N} \rho_i^2(k)\right)^i}{i!}\right)^{M-1} e^{-\sum_{i=1}^{N} \rho_i^2(k)} \cdot \left(\prod_{i=1}^{N} \rho_i(k)\right) d\rho_1(k) \cdots d\rho_N(k) d\theta \cdot \quad (4.31)$$

To simplify (4.31), we use the fact that if $g(v) = 1 - e^{-v} \sum_{i=0}^{N-1} \frac{v^i}{i!}$, then $g(v) \geq e^{-v} \frac{v^N}{N!}$ [11]. This yields,

$$P(\mathbf{c} \rightarrow \mathbf{e}) \geq \frac{1}{\pi} \int_0^{\frac{\pi}{2}} \prod_{k=1}^{K} M 2^N \int_0^{\infty} \cdots \int_0^{\infty} e^{\left(-\frac{E_s}{8N_0 \sin^2\theta} \sum_{i=1}^{N} \rho_i^2(k) \lambda_{ii}(k) \right)}$$
$$\cdot e^{-\sum_{i=1}^{N} \rho_i^2(k)} \left(\frac{e^{-\sum_{i=1}^{N} \rho_i^2(k)}}{N!} \right)^{M-1} \left(\sum_{i=1}^{N} \rho_i^2(k) \right)^{N(M-1)}$$
$$\cdot \left(\prod_{i=1}^{N} \rho_i(k) \right) d\rho_1(k) \cdots d\rho_N(k) d\theta. \quad (4.32)$$

With the help of the change of variable $u_i(k) = \rho_i^2(k)$ and implementing some mathematical manipulations, we can simplify (4.32) as

$$P(\mathbf{c} \rightarrow \mathbf{e}) \geq \frac{1}{\pi} \int_0^{\frac{\pi}{2}} \left(\frac{M}{(N!)^{M-1}} \right)^K$$
$$\cdot \prod_{k=1}^{K} \left(\sum_{i_1=1}^{N} \cdots \sum_{i_{(M-1)N}=1}^{N} \frac{\prod_{i=1}^{N} q_i!}{\prod_{j=1}^{N} \left(M + \frac{\lambda_j(k) E_s}{8N_0 \sin^2\theta} \right)^{q_j+1}} \right) d\theta. \quad (4.33)$$

Given that $A(k)$ has $r(k)$ non-zero eigenvalues, it is possible to express (4.33) as

$$P(\mathbf{c} \to \mathbf{e}) \geq \frac{1}{\pi} \int_0^{\frac{\pi}{2}} M^{\sum_{k \in \psi(\mathbf{c},\mathbf{e})} r(k)} \left(\frac{1}{M^{MN-1}(N!)^{M-1}} \right)^K \cdot \prod_{k \in \psi(\mathbf{c},\mathbf{e})} \left(\sum_{i_1=1}^{N} \cdots \sum_{i_{(M-1)N}=1}^{N} \frac{\prod_{i=1}^{N} q_i!}{\prod_{j=1}^{r(k)} \lambda_j^{q_j'+1}(k)} \left(\frac{E_s}{8MN_0 \sin^2\theta} \right)^{-\sum_{j=1}^{r(k)} q_j'} \right) \cdot \prod_{k \notin \psi(\mathbf{c},\mathbf{e})} \left(\prod_{i=1}^{N} q_i! \right) \left(\frac{E_s}{8N_0 \sin^2\theta} \right)^{-\sum_{k \in \psi(\mathbf{c},\mathbf{e})} r(k)} d\theta, \quad (4.34)$$

which in turn, at a sufficiently large SNR, can be written as

$$P(\mathbf{c} \to \mathbf{e}) \geq \frac{M^{\sum_{k \in \psi(\mathbf{c},\mathbf{e})} r(k)}}{\pi} \left(\frac{1}{M^{MN-1}(N!)^{M-1}} \right)^K \prod_{k \notin \psi(\mathbf{c},\mathbf{e})} \left(\prod_{i=1}^{N} q_i! \right) \cdot \int_0^{\frac{\pi}{2}} \prod_{k \in \psi(\mathbf{c},\mathbf{e})} \left(\left(\prod_{j=1}^{r(k)} \lambda_j^{-1}(k) \right) \sigma_1'(k,0) \left(\frac{1}{\sin^2\theta} \right)^{-\sum_{j=1}^{r(k)} q_j'} \right) \left(\frac{1}{2\sin^2\theta} \right)^{-\sum_{k \in \psi(\mathbf{c},\mathbf{e})} r(k)} d\theta \cdot \left(\frac{E_s}{4N_0} \right)^{-\sum_{k \in \psi(\mathbf{c},\mathbf{e})} r(k)}, \quad (4.35)$$

where $\sigma_1'(k,z)$ is the summation of the SNR terms with the same exponent. The upper bound in (4.29) and the lower bound in (4.35) suggest that the PEP is bounded between two curves that have the same slope. Based on this result, we argue that the actual pairwise error probability has the same slope as well, which is $\sum_{k \in \psi(\mathbf{c},\mathbf{e})} r(k)$.

Therefore, employing antenna selection reduces the diversity order of the system from $M\sum_{k\in\psi(\mathbf{c},\mathbf{e})} r(k)$ to $\sum_{k\in\psi(\mathbf{c},\mathbf{e})} r(k)$.

4.4.2 Selecting the Best Receive Antenna ($L > 1$)

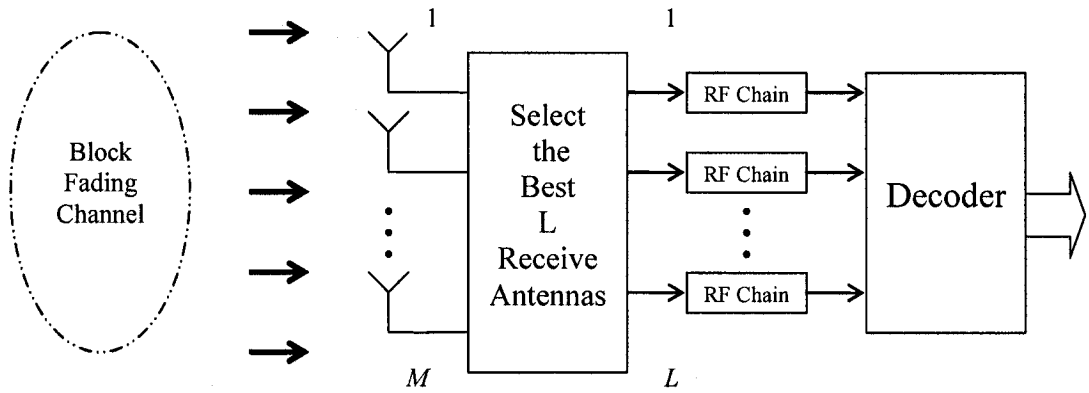

Figure 4.8: Antenna selection system, selecting the best L antennas.

For a system that selects the best L antennas (see Fig. 4.8), we can express the conditioned PEP defined by (4.2) as

$$P\left(\mathbf{c} \rightarrow \mathbf{e} \mid \Phi_1(k), \cdots, \Phi_L(k), k \in \{1, 2, \ldots, K\}\right) \leq e^{\left(-\sum_{k=1}^{K}\sum_{j=1}^{L}\left(\Phi_j(k)A(k)\Phi_j^*(k)\right)\frac{E_s}{4N_0}\right)}, \quad (4.36)$$

where it is assumed that $\|\Phi_1(k)\|^2 \geq \cdots \geq \|\Phi_L(k)\|^2$, and $\Phi_j(k)$ is the vector of N complex Gaussian random variables corresponding to the receive antenna with the j^{th} largest instantaneous SNR. To find an expression for the PEP, we average (4.36)

with respect to $\Phi_1(k), \ldots, \Phi_L(k)$ whose joint pdf is given as [45]

$$f_{\Phi_1(k),\ldots,\Phi_L(k)}(\phi_1(k), \ldots, \phi_L(k)) = \frac{M!}{\pi^{NL}(M-L)!L!L} e^{-\sum_{j=1}^{L}\|\phi_j(k)\|^2} \cdot \left(\sum_{q=1}^{L} \left(1 - e^{-\|\Phi_q(k)\|^2} \sum_{i=0}^{N-1} \frac{\|\phi_L(k)\|^{2i}}{i!} \right)^{M-L} I_{\Phi_q}(\phi_1(k), \ldots, \phi_L(k)) \right), \quad (4.37)$$

where $I_{\Phi_q}(\phi_1(t), \ldots, \phi_L(t)) = 1$ if $\phi_1(t), \ldots, \phi_L(t) \in \Phi_q$ and 0 otherwise. Due to the fact that for this case the derivation follows the case $L = 1$, to avoid repetition, we just give the main results. Using similar arguments that led to (4.26), we obtain

$$P(\mathbf{c} \to \mathbf{e}) \leq \prod_{k=1}^{K} \frac{M!}{(M-L)!L!(N!)^{M-L}} \cdot \left(\sum_{i_1=1}^{N} \cdots \sum_{i_{(M-L)N}=1}^{N} \frac{q_1!q_2!\cdots.q_N!}{\left(1+\lambda_1(k)\frac{E_s}{4N_0}\right)^{q_1'+1} \left(1+\lambda_2(k)\frac{E_s}{4N_0}\right)^{q_2'+1} \cdots \left(1+\lambda_{r(k)}(k)\frac{E_s}{4N_0}\right)^{q_{r(k)}'+1}} \right) \cdot \left(\frac{1}{\left(1+\lambda_1(k)\frac{E_s}{4N_0}\right)\left(1+\lambda_2(k)\frac{E_s}{4N_0}\right)\cdots\left(1+\lambda_{r(k)}(k)\frac{E_s}{4N_0}\right)} \right)^{L-1}. \quad (4.38)$$

At a sufficiently high SNR, (4.38) can be expressed as

$$P(\mathbf{c} \to \mathbf{e}) \leq \left(\frac{M!}{(M-L)!L!(N!)^{M-L}} \right)^{K} \cdot \prod_{k \in \psi(\mathbf{c},\mathbf{e})} \left(\left(\prod_{j=1}^{r(k)} \lambda_j^{-1}(k) \right)^{L-1} \sigma_L(k,0) \right) \cdot \prod_{k \notin \psi(\mathbf{c},\mathbf{e})} \left(\prod_{i=1}^{N} q_i! \right) \left(\frac{E_s}{4N_0} \right)^{-L \sum_{k \in \psi(\mathbf{c},\mathbf{e})} r(k)}, \quad (4.39)$$

where $\sigma_L(k,z)$ has a similar definition as that given in (4.28). The expression (4.39) suggests that the diversity order of the system is $L\sum_{k\in\psi(\mathbf{c},\mathbf{e})} r(k)$. By comparing this diversity order with that of the full-complexity system (see (4.12)), it is clear that employing antenna selection deteriorates the diversity order and reduces it from $M\sum_{k\in\psi(\mathbf{c},\mathbf{e})} r(k)$ to $L\sum_{k\in\psi(\mathbf{c},\mathbf{e})} r(k)$. Similar to the $L=1$ case, we still need a lower bound to confirm the diversity order suggested by the upper bound in (4.39). Again, to avoid repetition, we bring here just the main results. After some mathematical implementation, similar to what we did in Chapter 3 for the case $L>1$, we obtain

$$P(\mathbf{c}\rightarrow\mathbf{e}) \geqslant \frac{1}{\pi}\int_0^{\frac{\pi}{2}} \prod_{k=1}^{K} \frac{M!}{(M-L)!L!(N!)^{M-L}} \cdot \left(\sum_{i_1=1}^{N}\cdots\sum_{i_{(M-L)N}=1}^{N} \frac{\prod_{i=1}^{N} q_i!}{\prod_{i=1}^{N}\left(M-(L-1)+\lambda_i(k)\frac{E_s}{8N_0\sin^2\theta}\right)^{q_i+1}} \right) \cdot \prod_{i=1}^{N}\left(1+\lambda_i(k)\frac{E_s}{8N_0\sin^2\theta}\right)^{-(L-1)} d\theta. \quad (4.40)$$

Given that the SNR is high enough, the expression in (4.40) can be simplified as

$$P(\mathbf{c} \to \mathbf{e}) \geqslant \frac{1}{\pi} \int_0^{\frac{\pi}{2}} \left(\frac{M!}{(M-L+1)^{N(M-L+1)} (M-L)! L! (N!)^{M-L}} \right)^K \cdot \prod_{k \notin \psi} \left(\prod_{i=1}^{N} q_i! \right) \prod_{k \in \psi} \left(\prod_{i=1}^{r(k)} \lambda_i(k)^{-(L-1)} \right) \cdot \prod_{k \in \psi} \left(\sum_{i_1=1}^{N} \cdots \sum_{i_{(M-L)N}=1}^{N} \frac{\prod_{i=1}^{N} q_i!}{\prod_{i=1}^{r(k)} \lambda_i(k)^{q_i'+1}} \left(\frac{E_s}{(M-(L-1)) 8 N_0 \sin^2 \theta} \right)^{-\sum_{j=1}^{r(k)} q_j'} \right) \cdot \left(\frac{E_s}{(M-(L-1)) 8 N_0 \sin^2 \theta} \right)^{-\sum_{k \in \psi} r(k)} \left(\frac{E_s}{8 N_0 \sin^2 \theta} \right)^{-(L-1) \sum_{k \in \psi} r(k)} d\theta. \quad (4.41)$$

Finally, after some more simplifications, we get

$$P(\mathbf{c} \to \mathbf{e}) \geq \frac{(M-(L-1))^{\sum_{k \in \psi(\mathbf{c},\mathbf{e})} r(k)}}{\pi} \cdot \left(\frac{M!}{(M-L+1)^{N(M-L+1)} (M-L)! L! (N!)^{M-L}} \right)^K \int_0^{\frac{\pi}{2}} \prod_{k \notin \psi(\mathbf{c},\mathbf{e})} \left(\prod_{i=1}^{N} q_i! \right) \cdot \prod_{k \in \psi(\mathbf{c},\mathbf{e})} \left(\left(\prod_{i=1}^{r(k)} \lambda_i(k)^{-L} \right) \sigma_L'(k,0) \left(\frac{1}{\sin^2 \theta} \right)^{-\sum_{j=1}^{r(k)} q_j'} \right) \cdot \left(\frac{1}{2 \sin^2 \theta} \right)^{-L \sum_{k \in \psi(\mathbf{c},\mathbf{e})} r(k)} d\theta \left(\left(\frac{E_s}{4 N_0} \right)^{-L \sum_{k \in \psi(\mathbf{c},\mathbf{e})} r(k)} \right), \quad (4.42)$$

where $\sigma'_L(k,z)$ and z have the same definitions as those given in (4.39). The diversity order suggested by (4.42) confirms the diversity order suggested by (4.39). For comparison purposes, we list in Table 4.1 the diversity order for fast, block and slow fading channels for various scenarios. The results are given for both cases of the full-complexity and antenna selection systems.

Table 4.1: Diversity Order for Various Fading Channel.

Fading	*Block Length*	*Full − Complexity*	$L=1$	$L>1$
Fast	1	μM	μ	μL
Block	$1<\delta<l$	$M\sum_{k\in\psi(\mathbf{c},\mathbf{e})} r(k)$	$\sum_{k\in\psi(\mathbf{c},\mathbf{e})} r(k)$	$L\sum_{k\in\psi(\mathbf{c},\mathbf{e})} r(k)$
Slow	l	MN	MN	MN

4.5 Numerical Examples and Simulation Results

In this section, we present some numerical examples and simulation results to illustrate the results of this part of the work by using two STTCs, namely, the 4-PSK, 4-state and the 8-PSK, 8-state codes, given in [4]. The trellis diagrams of these codes are given Chapter 3. The number of transmit antennas in all cases is $N = 2$. The length of a frame coming out of each transmit antenna is $l = 130$. In all cases, where applicable, antenna selection is done based on maximizing the received SNR.

4.5.1 Numerical Examples

As it has been discussed in Chapter 3, evaluating the average PEP is possible by averaging (4.2) over a large number of channel realizataions, assuming a particular

error event of a certain length, and then repeating the averaging over all possible error events of the same length. We consider systems with two transmit and two or three receive antennas. The STTC used for the numerical examples is the 4-PSK, 4-state code, presented in [4]. We consider error event lengths two and three because they are the ones that dominate the performance at high SNR. We also consider block length $\delta = 5$. In averaging (4.2), when the best L antennas are selected, $d^2(\mathbf{c}, \mathbf{e})$ is calculated as

$$d^2_{\max}(\mathbf{c}, \mathbf{e}) = \sum_{k=1}^{K} \sum_{j=1}^{L} \sum_{t=(k-1)\delta+1}^{k\delta} \Phi_j(k) C(t) \Phi_j^*(k), \tag{4.43}$$

where $C(t)_{pq} = (c_t^p - e_t^p)\overline{(c_t^q - e_t^q)}$, and $\Phi_1(k), \ldots, \Phi_L(k)$ were defined earlier in Section 4.4.2. The relationship between $A(k)$ and $C(t)$ is given by(4.7), where $A(k) = \sum_{t=(k-1)\delta+1}^{k\delta} C(t)$ and δ is the length of a faded block. Note that the values of j and entries of $\Phi_j(k)$ of different blocks are independent of each other and may change from one block to another. Therefore, if an error event starts in a block and ends in a different block, the values of channel gains, i.e., the entries of $\Phi_j(k)$, are different.

In Figs. 4.9 and 4.10, numerical results for the average PEP with different selection scenarios are given. In Fig. 4.9 the PEP results are shown for the case of $N = M = 2$ and error event lengths 2 and 3. Fig. 4.10 shows the average PEP results for error event lengths 2 and 3. and for the case of $N = 2$, $M = 3$. It is clear from the figures that the slopes of the curves are not the same before and after antenna selection. As the result, diversity order degrades with antenna selection.

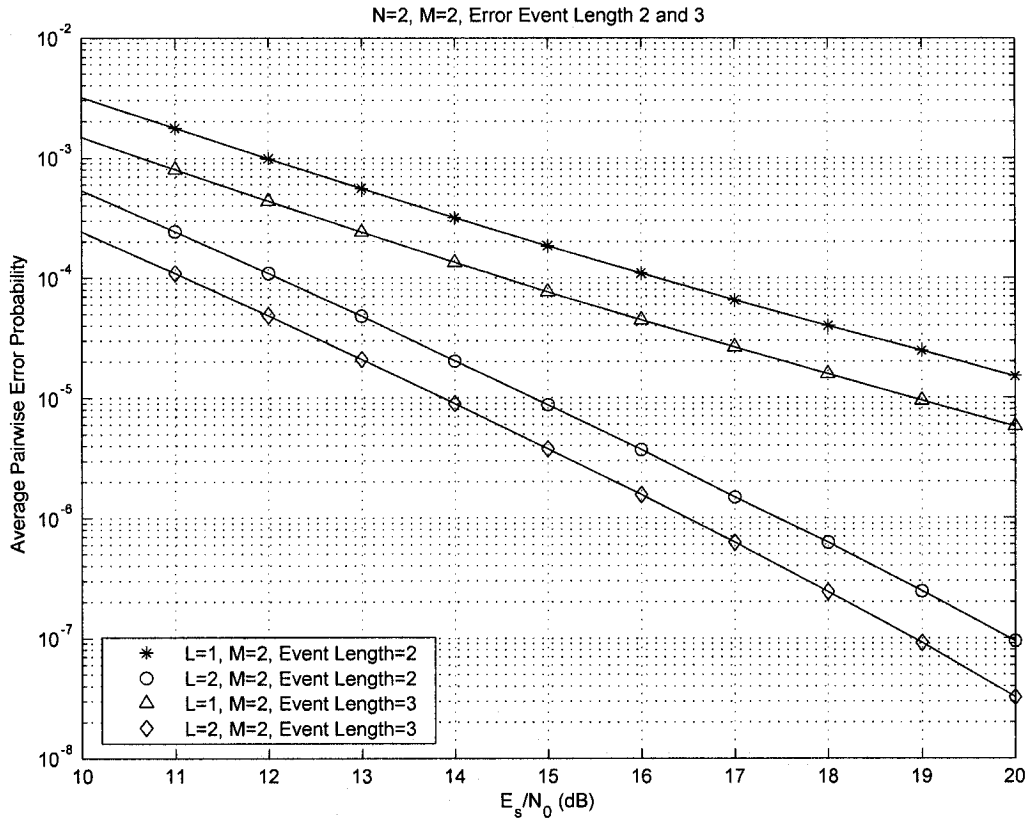

Figure 4.9: Average PEP for $M = 2$ and error event length 2 and 3, block length 5.

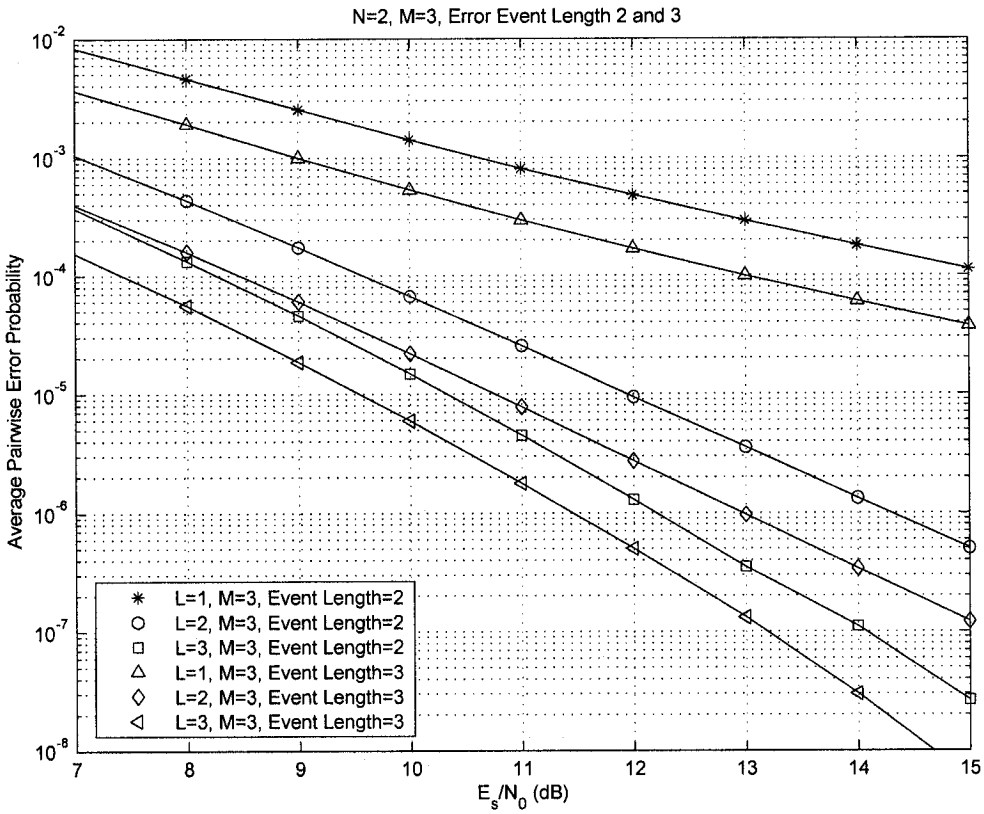

Figure 4.10: Average PEP for $M = 3$ and error event length 2 and 3, block length 5.

4.5.2 Simulation Results

In our simulations, we use the 8-PSK, 8-state code given in [4]. The number of transmit antennas for all cases is $N = 2$ and the number of receive antennas is 2 and 3. The fading channel considered is block Rayleigh fading with block lengths $\delta = 5$ and 13. The length of the frame is $l = 130$. In all cases, where applicable, the antenna selection is done based on maximizing the received SNR.

The results in Fig. 4.11 show the FER against the SNR in dB for various cases of antenna selection for $\delta = 5$. We observe from the figure that the slopes of the performance curves corresponding to different values of L, for a specific M, are different. This confirms that the diversity order deteriorates as a result of employing antenna selection. Moreover, the slopes of the performance curves corresponding to a specific L, for different values of M, are the same. In other words, the diversity order appears to be linearly proportional to L and it does not depend on M, which agrees with the analytical results derived in this work. On the other hand, as expected, increasing the number of receivers, for a specific L, provides additional coding gain. However, this additional coding gain becomes smaller as M increases.

In Fig. 4.12, we plot the FER for $\delta = 13$. As expected, increasing δ, for a specific M and different values of L, decreases the difference between the slopes of the FER curves. This can be explained as follows. First, increasing δ makes the channel behavior closer to that of a slow fading one. We know that employing antenna

selection over a slow fading channel does not degrade the diversity order. Thus, we expect that the slopes of the FER curves when δ is large to be closer to each other. Second, increasing δ decreases the number of blocks per frame and this decreases the probability of having error events extending over more than one block. Therefore, there will be fewer rank deficient block matrices, as compared to a channel with small δ.

In Fig. 4.13 and 4.14, the performance results for different block lengths and different selection scenarios are shown. In both figures, the number of selected antenna(s) remains the same, while the number of available antennas changes. In Fig. 4.13, system selects only the best antenna, while in Fig. 4.14, antenna selection system uses the two best antennas, for each block time duration. Results in these figures confirm that the diversity order of the STTC antenna selection system is a function of the number of selected antennas, which is in agreement with the mathematical results presented in this chapter.

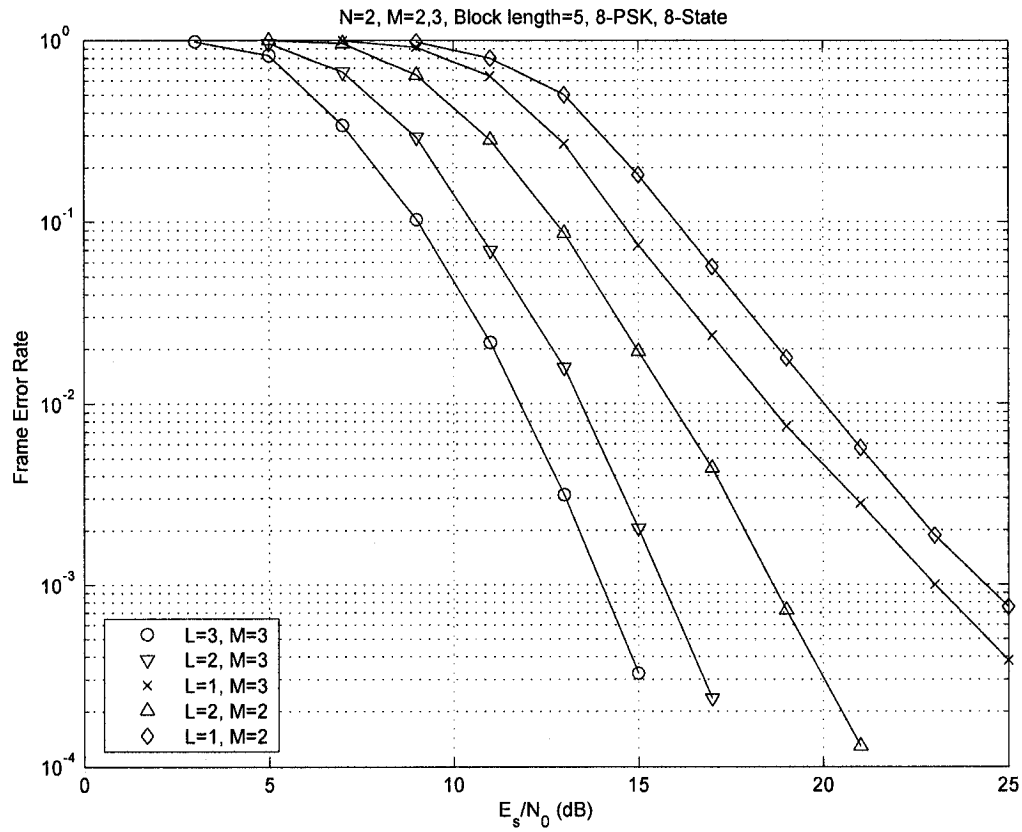

Figure 4.11: FER performance comparison between various antenna selection scenarios in block fading for block length 5 (8-PSK, 8-state).

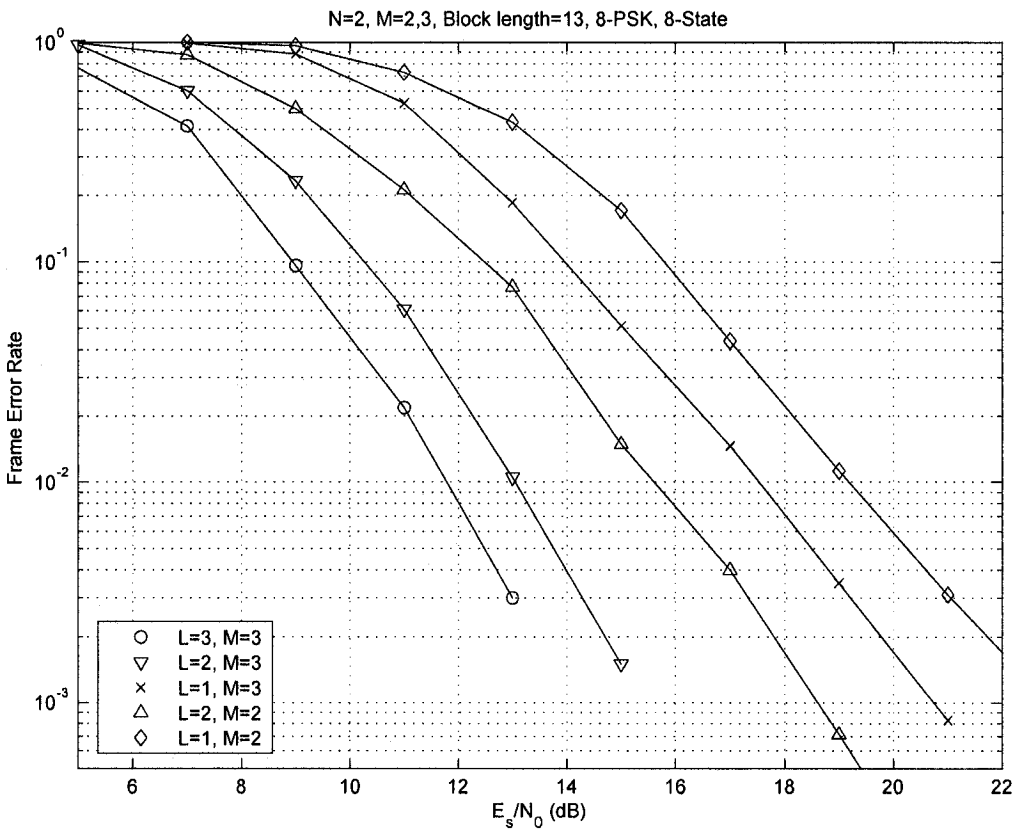

Figure 4.12: FER performance comparison between various antenna selection scenarios in block fading for block length 13 (8-PSK, 8-state).

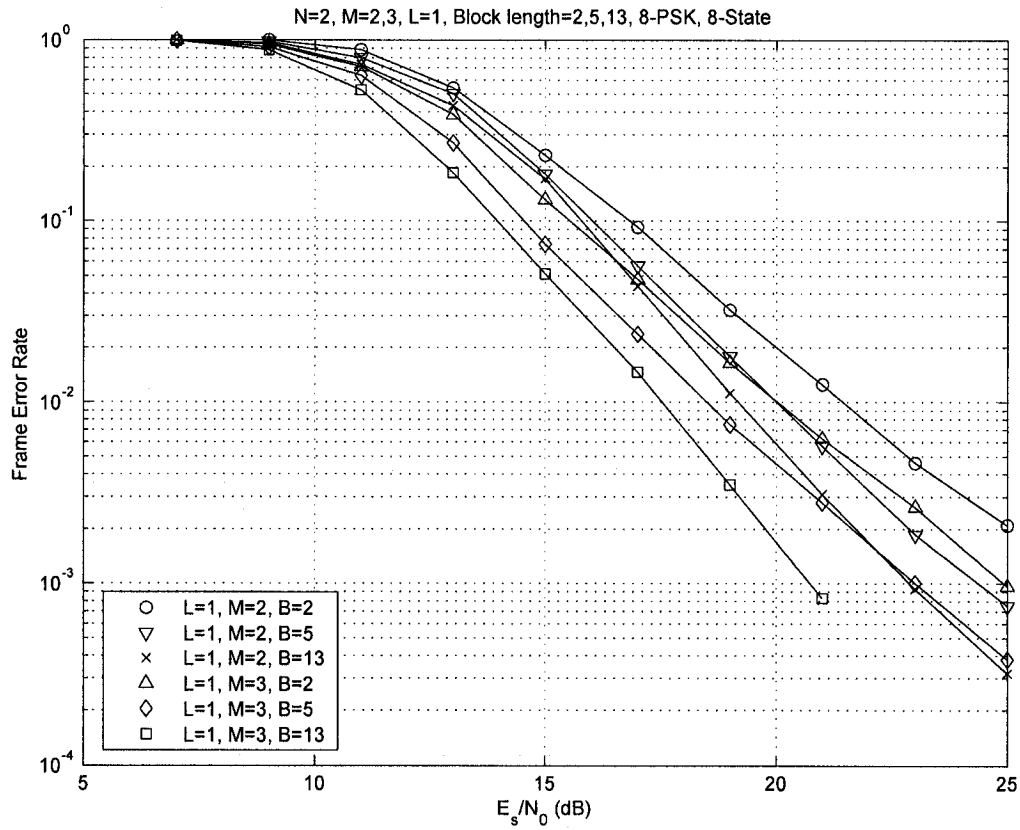

Figure 4.13: FER performance for different block length and for selecting the best antenna, block lengths 2, 5 and 13 (8-PSK, 8-state).

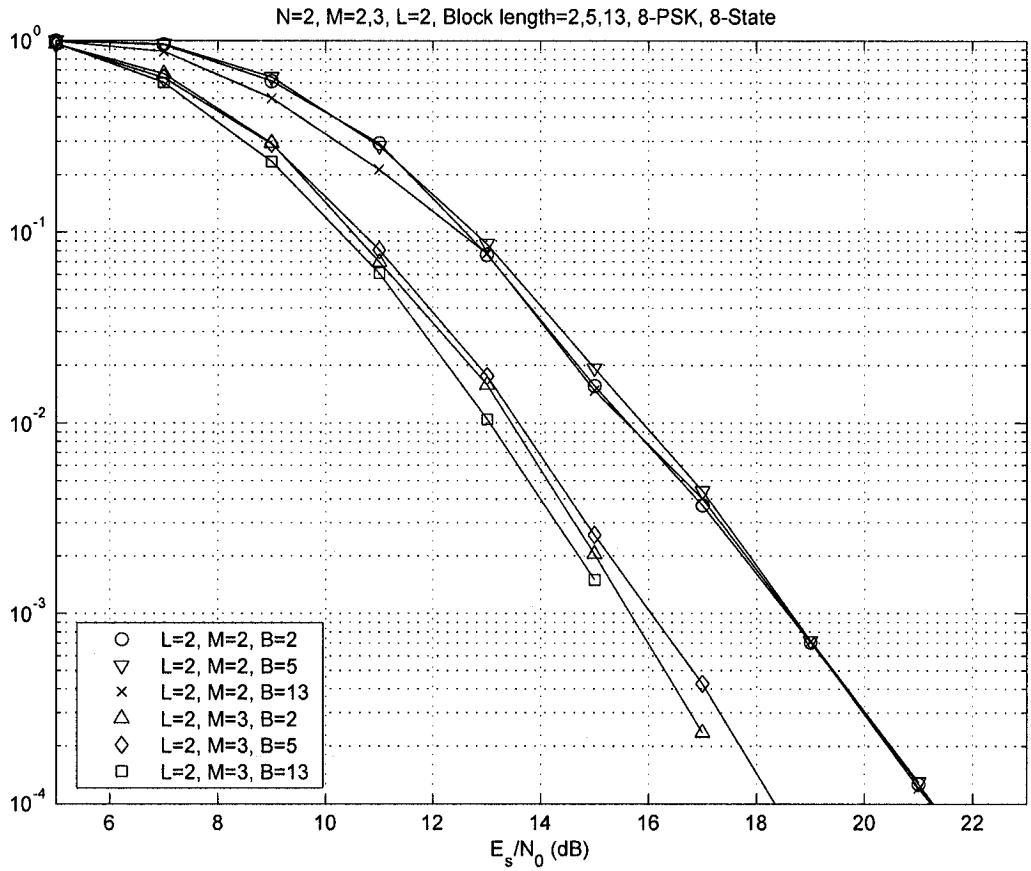

Figure 4.14: FER performance for different block length and for selecting two best antennas, block length 2, 5 and 13 (8-PSK, 8-state).

4.6 Conclusion

A thorough mathematical analysis was done to examine the performance of STTCs over block fading channels with antenna selection at the receiver side. Specifically, we derived explicit upper bounds on the PEP. Our analysis showed that employing antenna selection over block fading channels deteriorates the diversity order of the MIMO system and makes it linearly proportional to the number of selected antennas. As a result, increasing the total number of receive antennas in such systems increases the coding gain, but does not enhance the diversity order of the system. Our numerical examples and simulations results strongly supported the mathematical analysis.

The results for block fading channels are similar to those for fast fading channels and to slow fading channels when the underlying STTC is rank deficient. However, antenna selection does not affect the diversity order for orthogonal space-time block codes (STBCs) for all types of fading channels [39]. The same is true when a STBC is concatenated with an outer channel code, including TCM, convolutional and turbo codes [40]. These findings suggest that it may be more feasible to employ STBCs when antenna selection is considered, as opposed to STTCs.

Chapter 5

Conclusions and Future Work

5.1 Conclusions

5.1.1 Main Results

We have examined the performance of space-time trellis coded MIMO systems over fast Rayleigh fading channels with antenna selection at the receiver. We have adopted a selection criterion that is optimal in the sense of maximizing the received SNR. We have demonstrated that the diversity order degrades with antenna selection, and the resulting diversity order is linearly dependent on the number of selected antennas. This result is unlike the case of quasi-static fading where the diversity order is maintained with antenna selection. Our thorough mathematical analysis was supported through numerical examples and computer simulations.

In the second part of the thesis, a thorough mathematical analysis has been done to examine the performance of space-time trellis codes over block fading channels

with antenna selection at the receiver side. Our mathematical results are in full agreement with previous works, which are the two extreme cases of fast and slow fading channels. Moreover, our mathematical analysis, numerical examples and simulation results support each other. These results show that the impact of antenna selection on the diversity order depends upon the error event location. If some of the error events are extended over more than one block, some of the corresponding block matrices are likely to be rank deficient. Since error events occur randomly, there is no guarantee that the block matrices are all full rank and the system can be considered rank deficient. Based on this fact and through exact mathematical analysis, we showed that the diversity order of an antenna selection over block fading channel is not preserved and is linearly dependent on the number of selected antennas. Also, increasing the total number of available receiver antennas, while increases the coding gain of the system, does not enhance the diversity order of the MIMO system.

5.1.2 Intuitive Explanation

Although the degradation in diversity order due to antenna selection is counter-intuitive, in the following, we shall give an explanation as to why this result makes sense. A STTC is said to be full rank when the codeword difference matrix, or equivalently the matrix $C(t)$ in fast fading (or $A(k)$ for block fading) is full rank, where this rank normally equals the number of transmit antennas, N. Otherwise, the STTC is said to be rank deficient. Recall that when $t \in \varphi(\mathbf{c}, \mathbf{e})$ the matrix $C(t)$ always has rank 1 regardless of the number of transmit antennas, and thus the underlying STTC

code can be viewed as rank deficient. This implies that $N-1$ of the available transmit antennas do not provide any useful information to the receiver in terms of diversity gain.

As such, when antenna selection is performed, it is possible that the channel gains corresponding to these $N-1$ transmit antennas may lead to the selection of a 'bad' subset of the receive antennas. In such cases, although the selected antennas maximize the received SNR, in terms of diversity gain, it would be equivalent if these antennas were selected at random without any regard to SNR. Consequently, the resulting diversity order will depend on the number of selected antennas and not on the number of available antennas. Such events are those that dominate the asymptotic behavior of the PEP as they represent the worst case scenario. This argument holds for both fast and block fading channels.

5.1.3 STTCs Versus STBCs with Antenna Selection

In comparison with STTCs, STBCs have a low complexity advantage, but they do not provide any coding gain [6]. Therefore, a STBC, if considered, may need to be combined with an outer channel coding scheme in order to provide such coding gains [16], [17] and [51]. In some cases, it was demonstrated that a STBC used in conjunction with an outer channel code can be superior, in terms of performance, to a STTC at even a lower complexity [12]. In light of the results of this thesis and existing results in this area the conclusion is that, when antenna selection is considered, it is recommended to use STBCs when the channel is modeled as fast fading or block

fading with high mobility (or low data rate). On the other hand, it is recommended to use STTCs with antenna selection when the channel is modeled by quasi-static fading or block fading with low mobility (or high data rate).

5.2 Future Work

The following topics are deemed to be immediate extensions to our work.

5.2.1 Frequency Selective Fading

We only investigated the antenna selection over flat fading channels in our work. However, for high data rate wireless communication systems, the signal duration may be small compared to the multipath spread of the channel, resulting in a frequency-selective fading channel. It has been shown that for quasi-static frequency-selective fading, the maximum diversity gain is equal to DNM, where D is the number of resolvable multipath components and N, M are the number of transmit and receive antennas, respectively [50]. Recall that the diversity order for flat slow fading channel is NM. The authors in [49] used the idea of virtual antennas and considered frequency-selective slow fading as flat fading one, but with more antennas. As a result, it has been shown that, in a frequency-selective slow fading with antenna selection, one can still achieve full diversity provided that the underlying code is full-rank. Otherwise, the diversity order is reduced and it becomes a function of the number of selected antennas. The impact of antenna selection on frequency-selective block fading channel

(and fast fading channel, as a special case of block fading) has not been investigated yet and can be considered as future work. However, we believe that our results for flat fading extends in a straightforward manner to frequency selective fading.

5.2.2 Correlated Fading Channels

In most of the work on antenna selection, it has been assumed that the sub-channels fade independently. The implication of this assumption is that the adjacent antenna elements are placed far enough from each other so that they experience completely different fading. However, it may be difficult to satisfy this condition in practice, particularly when the wireless device is relatively small such that it is not possible to keep enough distance between adjacent antennas. Also, the assumption of independent fading no longer holds in an environment where scattering is not rich. It has been shown that for correlated quassi-static fading channel, the diversity order of the full-rank STTCs with antenna selection is the same as that of full-complexity one [23], whereas for the rank-deficient case the diversity order is not preserved and in fact it degrades.

The impact of antenna selection on correlated fast and block fading channels has not been investigated yet. However, considering the phenomenon investigated in Section 4.3.2, one can intuitively say that the diversity order of the STTC system with antenna selection system over block fading channel is not maintained, even if the code is full-rank. To investigate the accuracy of this intuition, we can extend this work and quantify the effect of channel correlation with antenna selection for various

cases of correlated fading channels.

5.2.3 Impact of Channel Estimation Error

In the analysis, it was assumed that the channel fading coefficients are perfectly known at the receiver. However, in real-world applications, such fading coefficients are estimated at the receiver. The impact of channel estimation error on the performance of space-time codes is still under investigation. So far, for example, it has been shown that with the increase of receive diversity, all STCs become more robust to channel estimation errors [52]. Moreover, for STTCs, as the number of trellis states increases, the codes become less robust to the channel estimation errors. For the case of antenna selection systems, the impact of channel estimation error on the performance of STTCs has not been investigated yet.

However, based on the fact that the estimation error can be modeled as a zero mean complex Gaussian random variable, we can intuitively say that the impact of channel estimation error may be considered as an increase in channel noise, which may result in a reduction in the system performance. This will be an interesting research topic to pursue.

5.2.4 Hardware Implementation

Employing antenna selection reduces the cost and complexity of MIMO systems. For example, the number of RF chains, as one of the most expensive part of the

system, reduces from M to L. However, the number of antennas and low-noise amplifiers (LNA), which come immediately after antennas, are the same as that of the full-complexity system. On the other hand, employing antenna selection requires using an RF switch. The RF switches available with current technologies are far from ideal, a fact that may offset some of the advantages of antenna selection. The most important shortcoming of the practical switches is their transfer attenuation, which must be compensated by more power from the output stage amplifier of the transmitter and by a more sensitive LNA at the receiver [43]. Therefore, investigating the saving that can be achieved with antenna selection in practice is an interesting topic to pursue.

Bibliography

[1] E. Telatar, "Capacity of multi-antenna Gaussian channels," AT&T Bell Labs Internal Memo., June 1995.

[2] G. Foschini and M. Gans, "On the limits of wireless communications in a fading environment when using multiple antenna," *Wireless Personal Communications*, vol. 6, no. 3, pp. 311-335, March 1998.

[3] J. C. Guey, M. P. Fitz, M. R. Bell, and W. Y. Kuo, "Signal design for transmitter diversity wireless communication systems over Rayleigh fading channels," *Proceeding, IEEE Vehicular Technology Conference*, vol. 1, pp. 136-140, 1996.

[4] V. Tarokh, N. Seshadri, and A. R. Calderbank, "Space-time codes for high data rate wireless communication: Performance criterion and code construction," *IEEE Transaction Information Theory*, vol. 44, pp. 744-765, March 1998.

[5] S. M. Alamouti, "A simple transmit diversity technique for wireless communications," *IEEE Journal on Selected Areas in Communications*, vol. 16, No. 8, pp. 1451-1458, Oct. 1998.

[6] V. Tarokh, H. Jafarkhani, and A. R. Calderbank, "Space-time block codes from orthogonal designs," *IEEE Transaction Information Theory*, vol. 45, no. 5, pp. 1456-1467, July 1999.

[7] A. R. Hammons, Jr. and H. El Gamal, "On the theory of space-time codes for PSK modulation," *IEEE Transaction Information Theory*, vol. 46, no. 2, pp. 524-542, March 2000.

[8] Q. Yan and R. S. Blum, "Optimum space-time convolutional codes," *Proceeding, IEEE Wireless Communications and Networking Conference*, vol. 3, pp. 1351-1355, 2000.

[9] S. Baro, G. Bauch, and A. Hansmann, "Improved codes for space-time trellis-coded modulation," *IEEE Communication Letters*, vol. 4, no. 1, pp. 20-22, January 2000.

[10] Y. Liu, M. P. Fitz, and O. Y. Takeshita, "Full rate space-time turbo codes," *IEEE Journal on Selected Areas in Comm.*, vol. 19, no. 5, pp. 969-980, May 2001.

[11] A. Stefanov and T. M. Duman, "Turbo coded modulation for systems with transmit and receive antenna diversity over block fading channels: System model, decoding approaches and practical considerations," *IEEE Journal on Selected Areas in Communications*, vol. 19, No. 5, pp. 958-968, May 2001.

[12] S. Sandhu, R. Heath, and A. Paulraj,"Space-time block codes versus space-time trellis codes," *Proceeding, IEEE International Conference on Communication (ICC),* vol. 4, pp. 11-14, June 2001.

[13] S. M. Alamouti, V. Tarokh, and P. Poon, "Trellis-coded modulation and transmit diversity: design criteria and performance evaluation," *Proceeding, IEEE International Conference on Universal Personal Communication (ICUPC),* vol. 1, pp. 703-707, 1998.

[14] S. Baro, G. Bauch, and A. Hansmann,"Improved codes for space-time trellis-coded modulation," *IEEE Commun Letters,* vol. 4, no. 1, pp. 20-22, January 2000.

[15] Y. Liu, M. P. Fitz, and O. Y. Takeshita, "Full rate space-time turbo codes," *IEEE Journal on Selected Areas in Communication,* vol. 19, no. 5, pp. 969-980, May 2001.

[16] Y. Gong and K. B. Letaief, " Concatenated space-time block coding with trellis coded modulation in fading channels," *IEEE Transaction Wireless Communications,* vol. 1, no. 4, pp. 580-590, Oct. 2002.

[17] A. Yongacoglu, and M. Siala, "Space-time codes for fading channels," *IEEE Transaction Vehicular Technol.,* vol. 5, pp. 2495-2499, Sept. 1999.

[18] D. Gore and A. Paulraj, "Statistical MIMO antenna sub-selection with space-time coding," *Proceeding, IEEE International Con. on Communication (ICC)*, vol. 1, pp. 641-645, 2002.

[19] D. Gore, R. U. Nabar, and A. Paulraj, "Selecting an optimal set of transmit antennas for a low rank matrix channel," *Proceeding, IEEE International Conference on Acoustics, Speech and Signal Processing (ICASSP)*, pp. 2785-2788, 2000.

[20] R. W. Heath, S. Sandhu, and A. Paulraj, "Antenna selection for spatial multiplexing systems with linear receivers," *IEEE Communication Letters*, vol. 5, no. 4, pp. 142-144, April 2001.

[21] A. Ghrayeb and T. M. Duman, "Performance analysis of MIMO systems with antenna selection over quasi-static fading channels," *IEEE Transaction on Vehicular Technology*, vol. 52, no. 2, pp. 281-288, March 2003.

[22] I. Bahceci, T. M. Duman, and Y. Altunbasak, "Antenna selection for multiple-antenna transmission systems: Performance analysis and code construction," *IEEE Transaction on Information Theory*, vol. 49, no. 10, pp. 2669-2681, Oct. 2003.

[23] I. Bahceci, Y. Altunbasak and T. Duman, "Space-time coding over correlated fading channels with antenna selection," *IEEE International Conference on Communications*, vol. 2, pp. 832-836, Jun. 2004.

[24] A. Gorokhov, D. A. Gore, and A. J. Paulraj, "Receive antenna selection for MIMO spatial multiplexing: theory and algorithms," *IEEE Transaction Signal Processing*, vol. 51, no. 11, pp. 2796-2807, Nov. 2003.

[25] A. Gorokhov, D. A. Gore, and A. J. Paulraj, "Receive antenna selection for MIMO flat-fading channels: theory and algorithms," *IEEE Transaction Information Theory*, vol. 49, no. 10, pp. 2687-2696, Oct. 2003.

[26] C. Zhuo, B. Vucetic, and Y. Jinhong, "Space-time trellis codes with transmit antenna selection," *IEE Electronics Letters*, vol. 39, no. 11, pp. 854-855, May 2003.

[27] A. F. Molisch and X. Zhang, "FFT-based hybrid antenna selection schemes for spatially correlated MIMO channels," *IEEE Communication Letters*, vol. 8, no. 1, pp. 36-38, Jan. 2004.

[28] A. F. Molisch, M. Z. Win, and J. H. Winters, "Capacity of MIMO systems with antenna selection," *Proceeding, IEEE International Conference on Communications (ICC)*, vol. 2, pp. 570-574, June 2001.

[29] R. S. Blum and J. H. Winters, "On optimum MIMO with antenna selection," *IEEE Communication Letters*, vol. 6, no. 8, pp. 322-324, Aug. 2002.

[30] R. S. Blum, "MIMO capacity with antenna selection and interference," *Proceeding, IEEE International Conference on Acoustics, Speech and Signal Processing (ICASSP)*, vol. 4, April 2003, pp. 824-827.

[31] C. Zhuo, Y. Jinhong, B. Vucetic, and Z. Zhendong "Performance of Alamouti scheme with transmit antenna selection," *IEE Electronics Letters*, vol. 39, no. 23, pp. 1666-1668, Nov. 2003.

[32] H. W. Wing and E. G. Larsson, "Orthogonal space-time block coding with antenna selection and power allocation," *IEE Electronics Letters*, vol. 39, no. 4, pp. 379-381, Feb. 2003.

[33] L. C. Tran, T. A. Wysocki and A. Mertins, "Improved antenna selection technique to enhance the downlink performance of mobile communications systems," *Proceeding, 7th International Symposium on Signal Processing and Its Applications (ISSPA 2003),* Paris, France, 1-4, July 2003.

[34] Dhananjay A. Gore and Arogyaswami J. Paulraj, "MIMO antenna subset selection with space-time coding," *IEEE Transaction on Signal Processing*, vol. 50, no. 10, pp. 2580-2588, Oct. 2002.

[35] C. Zhuo, Y. Jinhong, B. Vucetic, and Z. Zhendong,"Space-time trellis codes with transmit antenna selection," *IEE Electronic Letters,* vol. 33, no. 11, pp. 854-855, May 2003.

[36] S. W. Kim and E. Y. Kim, "Optimum receive antenna selection minimizing error probability", *IEEE Wireless Communications and Networking Conference (WCNC 2003)* , no. 1, Mar 2003 pp. 441-447

[37] M. Katz, E. Tiirola, and J. Ylitalo, "Combining space-time block coding with diversity antenna selection for improved downlink performance," *Proceeding, IEEE Vehicular Technology Conference*, pp. 178-182, 2001.

[38] D. A. Gore and A. Paulraj, "MIMO antenna subset selection with space-time coding," *IEEE Transaction on Sig. Proc.*, vol. 50, no. 10, pp. 2580-2588, Oct. 2002.

[39] X. Zeng and A. Ghrayeb, "Performance bounds for space-time block codes with receive antenna selection," *IEEE Transactions on Information Theory, vol.* 50, no. 9, pp. 2130-2137, September 2004.

[40] X. Zeng and A. Ghrayeb, "Performance bounds for combined channel coding and space-time block coding with antenna selection," accepted for publications in *IEEE Transactions on Vehicular Technology* (November 2005).

[41] X. Nian Zeng and Ali Ghrayeb, "Antenna selection for space-time block codes over correlated Rayleigh fading channels," *IEEE Canadian Journal of Electrical and Computer Engineering (CJECE),* vol. 29, no. 4, pp. 219-226, October 2004.

[42] A. Goldsmith, Wireless Communications, Cambridge University Press, 2005.

[43] S. Sanayei and A. Nosratinia, "Antenna selection in MIMO systems," *IEEE Communications Magazine*, vol. 42, no. 10, pp. 68-73, Oct. 2004.

[44] R. A. Horn and C. R. Johnson, *Matrix Analysis.* New York: Cambridge University Press, 1988.

[45] B. C. Arnold, N. Balakrishnan, and H. N. Nagaraja, *A First Course in Order Statistics*, Wiley-Inetrscience, 1993.

[46] H. El. Al Gamal and A. R. Hammons, Jr.,"On the Design of Algebraic Space-Time Codes for MIMO Block-Fading Channels," *IEEE Transaction on Inform. Theory,* vol. 49, pp 151-163, Jan. 2003.

[47] J. W. Craig,"A new, simple, and exact result for calculating the probability of error for two-dimensional signal constellations," *Proceeding, IEEE Military Communication Conference (MILCOM)*, McLean, VA, pp. 571-575, Oct. 1991.

[48] B. Vucetic and J. Yuan, Space-Time Coding, John Wiley & Sons, 2003.

[49] T. Gucluoglu, T. Duman and A. Ghrayeb," Antenna selection for space-time coding over frequency-selective fading channel," *IEEE International Conference on Acoustics, Speech and Signal Processing (ICASSP),* vol. 4, pp. iv-709– iv-712, May 2004.

[50] M. Qin and R. Blum," Properties of space-time codes for frequency-selective channels," *IEEE Transaction on Signal Processing,* vol. 52, no. 3, pp 694-702, Mar. 2004.

[51] G. Kang, X. Jin, Q. Quan, P. Zhang," The decision schemes on the concatenation of space-time block code and convolutional code in WCDMA system," *International Conferences on Info-tech and Info-net,* vol. 2, pp. 693 - 697, 29 Oct.-1 Nov. 2001.

[52] Z. Diao, D. Shen and V. O. K. Li," Performance analysis of space-time codes with channel information errors," *IEEE 60th Vehicular Technology Conference,* vol. 4, pp. 26-29, Sept. 2004.